Searches for New Physics at the Large Hadron Collider

Jeffrey D. Richman

Abstract The experiments currently underway at the Large Hadron Collider are exploring the physics of the TeV energy scale, which may hold the answers to some of the most profound questions in particle physics. These lectures describe the status of searches for new physics beyond the standard model, focusing on supersymmetry, but addressing other aspects of this enormously broad physics program as well. Such topics as extra spatial dimensions, new gauge bosons, and microscopic black holes are included in the category known as exotica; some of these possibilities are also considered here. The methodologies and challenges associated with searches for new physics are discussed, followed by a survey of some of the basic phenomenology and the experimental results. This pedagogical review is intended for graduate students and postdocs who are working on this critical part of the LHC research program.

1 Introduction

I am delighted to be here at St. Andrews University, a distinguished six-hundred-year-old institution, to present lectures on searches for new physics at the Large Hadron Collider (LHC). The current period is one of intensive effort to explore the physics of the TeV energy scale, which may allow us to address some of the most fundamental mysteries of nature. Figure 1 shows a conception of the particle physics landscape, both known and speculative, by Sergio Cittolin, a fellow member of CMS. We are all privileged as scientists to be able to use one of the most extraordinary scientific instruments of all time – the LHC – to explore the unknown territory of the TeV scale.

Jeffrey D. Richman
Department of Physics, University of California, Santa Barbara, CA, 93106, e-mail: richman@hep.ucsb.edu

Fig. 1 A view of the LHC particle physics landscape by Sergio Cittolin, in the style of Leonardo da Vinci. Figure used with permission.

In these lectures, I adopt an unashamedly pedagogical approach. My goal is to explain as many simple things as possible, to focus on topics that I find interesting and fun, and not to worry about being comprehensive and balanced, as one would be in a review talk at a conference. I have tried to avoid covering results and ideas that are explained by other speakers at this school. Peter Maettig has done an admirable job of describing many important new physics searches in the context of his lectures on standard model (SM) results from the LHC experiments. Giacomo Cacciapaglia and Sven Heinemeyer have presented beautiful lectures on theoretical aspects of new physics. Bill Murray has summarized the amazing experimental results from the Higgs searches. For an excellent discussion of statistical issues, the reader is referred to the lectures by Glen Cowan. My own presentation is shaped by my involvement in supersymmetry searches in the CMS experiment, but I have tried to use examples from ATLAS as well.

2 Key Problems and Puzzles at the Electroweak Scale

This is a special year for physics and for the Scottish Universities Summer School in Physics. The discovery of a new particle [1, 2] with mass $m \approx 125$ GeV and properties consistent with those of a Higgs boson is an historic achievement. We are honored to have Peter Higgs with us here to speak about the deep insights that he, Robert Brout, Francois Englert, and other theorists developed some 50 years ago [3, 4, 5, 6]. These ideas have provided invaluable guidance to our field, and they have helped us to develop powerful experimental tools and methods needed for this remarkable discovery, especially the ATLAS [7] and CMS [8] detectors.

Given that the new particle decays to $\gamma\gamma$ and ZZ, it must be a boson. Furthermore, a spin-1 particle cannot decay into two photons [9], so the new particle cannot be another massive, spin-1 gauge boson, like the Z. Assuming that the Higgs hypothesis is confirmed by ongoing measurements, the particle will be the first fundamental scalar particle observed in nature (there are, of course, mesons with the quantum numbers $J^{PC} = 0^{++}$ [10]). We are thus on the verge of confirming the mechanism of electroweak symmetry breaking, in which the properties of the vacuum play a crucial role in explaining how massive gauge bosons can be accommodated in a gauge theory without destroying gauge invariance. And in the unlikely scenario in which the new particle turns out not to be a Higgs boson, we will be in a state of complete confusion, which will be even more interesting!

The observation of this new Higgs-like particle suggests strongly that we are on the right track conceptually in particle physics. We have found a new puzzle piece, and it appears to fit perfectly! But while it may turn out that the SM is nominally complete, the discovery certainly does not come close to resolving all of the many profound mysteries of our field.

Although the Higgs sector helps us to understand the origin of fundamental particle masses in a gauge theory, the low mass of the new particle itself presents a puzzle, which has been anticipated for some time. This is the gauge hierarchy problem [11], and it is inextricably bound up with the spin-0 nature of the Higgs boson. The squares of the bare masses (m^0) of fundamental scalar particles generically receive radiative corrections from quantum loop effects that depend quadratically on the cutoff scale Λ for momenta in the loop. In the case of the Higgs boson (h),

$$m_h^2 = (m_h^0)^2 + \Delta m_h^2 \tag{1}$$

and in the SM, the one-loop corrections are [12]

$$\Delta m_h^2 \simeq -\frac{3\Lambda^2}{8\pi^2 v^2}(4m_t^2 - 2M_W^2 - M_Z^2 - m_h^2), \tag{2}$$

where v is the Higgs vacuum expectation value. The contribution from the top-quark loop is dominant for light Higgs masses, and, barring a fine tuning of parameters to arrange cancellation of the loop effects, the Higgs mass is pulled to the scale Λ. If Λ corresponds to a high mass scale such as the reduced Planck scale $M_{\mathrm{Pl}} = \sqrt{\hbar c/(8\pi G_N)} \simeq 2.4 \times 10^{18}$ GeV, the degree of fine tuning required is severe, around 30 orders of magnitude. While such a cancellation is not excluded in principle, we are not aware of any physical reason for it to occur, and it seems highly unlikely that such a precise cancellation would occur by accident. This prediction is therefore regarded (by at least by some people) as unnatural. The criterion of *naturalness* is not straightforward to define, and various definitions have been given in the literature [13, 14]. Roughly speaking, the predictions of a natural theory should be stable with respect to small variations in its parameters. As discussed in the lectures by Giacomo Cacciapaglia in these proceedings, there are several possible avenues for stabilizing the mass hierarchy, including supersymmetry, extra dimensions, and technicolour. The discovery of a Higgs-like particle has actually given us more reason to search for new physics beyond the SM!

A perhaps more empirically based reason to search for new physics at the LHC is the compelling evidence for dark matter [15, 16, 17], which is known from astrophysical observations to dominate the matter density of the universe. The effects of dark matter are observed in several types of phenomena, including galactic rotation curves, anisotropies in the cosmic microwave background radiation, and microlensing observations. We should be humbled by the fact that, in spite of our excellent understanding of "ordinary" atomic matter (and its relatives in the second and third generations), the majority of the matter of the universe cannot be explained by the SM particle spectrum. To unravel this mystery, we need to detect cosmic dark matter directly, and we need to produce and study dark matter in detail. Ideally, the information from two lines of investigation—special low-background experiments and accelerator-based experiments—would then be combined, giving a full understanding of the physics of dark matter.

Supersymmetry (SUSY), which relates fermions and bosons, is a framework that, in a large range of scenarios, provides not only a solution to the gauge hierarchy problem, but also a dark-matter candidate. SUSY extends the Poincaré group of Lorentz boosts, rotations, and translations in a radical way, mapping bosonic and fermion degrees of freedom onto each other [11, 18, 19, 20, 21, 22, 23]. The quantum corrections to the Higgs-boson mass are greatly reduced by the presence of amplitudes associated with loop diagrams containing virtual SUSY particles, substantially cancelling the corresponding SM contributions [13]. Another attractive feature of SUSY is that it can lead to convergence of the running gauge coupling constants at high energy, which would be an indication that the physical laws of nature can be described (at high energies) by a unified gauge theory with a single gauge group and a single gauge coupling constant. If the SUSY partners exist at the weak scale, unification of the coupling constants can take place around $M_{\mathrm{GUT}} \sim 2 \times 10^{16}$ GeV. For all of these reasons, SUSY has acquired a somewhat special status as an extension to the SM. My own emotional state oscillates between awe at its fundamental beauty and deep implications on the one hand and, on the other, dismay at its complexity, particularly with regard to the breaking of supersymmetry. So many scenarios, so many parameters! But in the end, the only thing that matters is whether the theory describes the real world, not whether we think it is beautiful.

The range of new physics possibilities accessible at the LHC extends far beyond SUSY. The term *exotica*, which is used in both ATLAS and CMS as well as in the Tevatron experiments, encompasses a vast range of new particles and phenomena. These include resonances, such as heavy gauge bosons (W', Z'); compositeness of SM particles (substructure); 4th generation particles; leptoquarks (particles with both lepton and baryon quantum numbers); various scenarios leading to long-lived particles (including SUSY); microscopic black holes (motivated by ideas about TeV-scale gravity); heavy neutrinos; tests of triple gauge couplings; and contact interactions (resulting from the exchange of very heavy particles). It is impor-

Table 1 Broad categories for supersymmetry searches. The list is far from comprehensive, and many of the categories overlap.

Supersymmetry
R-parity conserving (E_T^{miss}-based searches)
R-parity violating (searches without the E_T^{miss} signature)
Inclusive searches for topological signatures (*e.g.,* for MSUGRA/cMSSM)
Searches for signature for gauge-mediated SUSY breaking
Searches for signatures with γ, Z
Searches motivated by naturalness considerations (light $\tilde{t}$, $\tilde{b}$, $\tilde{g}$, $\tilde{\chi}^{\pm}$, $\tilde{\chi}^0$)
Strong production of SUSY
Electroweak production of SUSY
Monojet events and connection to direct dark matter searches
Long-lived SUSY particles, *e.g.,* long-lived gluinos, R-hadrons
Split SUSY
Stealth SUSY

Table 2 A partial list of the main categories for exotica searches.

Exotica
Large extra dimensions
Universal extra dimensions
Randall-Sundrum models
Hidden valley models
Microscopic black holes
Contact interactions
New heavy gauge bosons
Leptoquarks
4th generation quarks and leptons
Excited quarks and leptons
Technihadrons
Heavy Majorana neutrinos
Heavy right-handed W bosons
Long-lived particles

tant to recognize that SUSY is not the only idea for addressing the gauge hierarchy problem. For example, Randall-Sundrum warped-extra-dimension models [24] and models with large extra dimensions [25] provide intriguing alternative perspectives. Some of these exotica searches, including the extremely important possibility of new heavy gauge bosons, arise naturally in the context of detailed or even precision studies of SM processes and are discussed in the lectures by Peter Maettig.

While these and other motivations for new physics searches are intriguing and even compelling, I would like to advocate that we not lose sight of another more basic perspective. This is simply that the TeV scale is, on empirical grounds, a critical energy scale of nature, and it may provide information that allows us to access physical laws operating at much higher mass scales. Looking back, it required several decades to explore and understand the physics accessible at the GeV scale. That scale yielded far more physics than anyone could have possibly imagined. In fact, the LHCb experiment is still pursuing many important questions in B and B_s meson physics, some of which have important implications for physics at higher mass scales. The TeV scale could require substantially more time and effort to understand than the GeV scale, and the LHC may not be able to provide all the answers. But it is our responsibility to exploit the full potential of the LHC as we explore this new territory.

These lectures consist of four main parts: methodological challenges and problems in searches for new physics (Section 4), characteristics of SM backgrounds (Section 5), searches for supersymmetry (Section 6), and searches for exotica, focusing on searches with unusual features and methods (Section 7).

3 References and Resources

Both ATLAS and CMS maintain web pages that enable one to quickly obtain an overview of the search results currently available. The starting points for obtaining ATLAS and CMS physics results are

- https://twiki.cern.ch/twiki/bin/view/AtlasPublic
- https://twiki.cern.ch/twiki/bin/view/CMSPublic/PhysicsResults

Results related to supersymmetry are linked to the following web pages:

- https://twiki.cern.ch/twiki/bin/view/AtlasPublic/SupersymmetryPublicResults
- https://twiki.cern.ch/twiki/bin/view/CMSPublic/PhysicsResultsSUS

Results related to exotica searches are linked to the following web pages:

- https://twiki.cern.ch/twiki/bin/view/AtlasPublic/ExoticsPublicResults
- https://twiki.cern.ch/twiki/bin/view/CMSPublic/PhysicsResultsEXO

There are also numerous review articles and books that can be extremely helpful to someone facing the daunting task of learning this physics. A time-honored resource is *A Supersymmetry Primer*, by S. P. Martin [23]. Several detailed books on supersymmetry with extensive discussions of phenomenology are also now available. *Supersymmetry in Particle Physics*, by I. Aitchison [26], is particularly helpful to beginners. Other books, such as *Weak Scale Supersymmetry*, by H. Baer and X. Tata [27], *Supersymmetry: Theory, Experiment, and Cosmology*, by P. Binétruy [12], and *Theory and Phenomenology of Sparticles*, by M. Drees, R. H. Godbole, and P. Roy [28], are more advanced and comprehensive. A standard text that has been used for many years is *Supersymmetry and Supergravity* by J. Wess and J. Bagger [29]. The *Review of Particle Properties* contains two reviews of supersymmetry, one theoretical (H. Haber) [11] and one experimental (Buchmuller and de Jong) [30], each of which provides a wealth of information and references. A valuable resource for understanding the ATLAS and CMS detectors is *At the Leading Edge: the ATLAS and CMS LHC Experiments*, edited by Dan Green [31].

4 Challenges in Searches for New Physics

There are many challenges in searching for new physics. The first part of this section, *Bumps in the Road* (Section 4.1), presents examples of searches that have run into difficulties, leading to conclusions that were not confirmed by later studies. In the second part, *Lessons Learned: Common Problems in Searches for New Physics* (Section 4.2), we consider what lessons can be learned from these struggles.

Here are some questions to think about:

- How well do you understand the detector systems and software that affect your measurement?
- Are there aspects of the analysis that are not validated by studies of control samples in the data? What is the weakest element of the analysis? Can this element be strengthened?
- If you observe an excess in your search, will you trust the systematic uncertainties and the significance or will you want to rethink them? What are the systematic uncertainties fundamentally based on?

And here are some provocative assertions to consider:

- The foundation of any search is a detailed understanding of the SM backgrounds.
- In a well-designed and executed analysis, one obtains a coherent physical picture of the event sample, including both the signal region and the surrounding neighborhood in the sample. This physical picture gives credibility to the results.
- In general, systematic uncertainties do not have a well-defined probability content. If they are comparable to (or larger than) the statistical uncertainties, the meaning of the total uncertainty becomes questionable.

4.1 Bumps in the Road

Searches for new particles or for new physical processes present both great opportunities and challenges. Historically, a significant number of searches in our field have enountered serious problems, and it is instructive to consider some of these and to see what lessons we can learn. Below we review examples of measurements that obtained conclusions that were later found to be incorrect. I will not, however, try to give a detailed explanation of what happened in each case –it is not always straightforward to obtain a clear picture from the published literature. I encourage you to read the papers and to develop your own ideas.

In 1984, the Crystal Ball experiment announced a preliminary result [32] (which was not published in a journal), "Evidence for a Narrow Massive State in the Radiative Decays of the Upsilon." The full process was $e^+e^- \to \Upsilon(1S) \to \gamma + \zeta(8.3)$, where $\zeta(8.3)$ was the name tentatively assigned to a new particle whose mass (8.3 GeV) was inferred from the location of the monochromatic peak in the energy spectrum of the recoiling photon. The $\Upsilon(1S)$ is a $b\bar{b}$ bound state with $L = 0$, $S = 1$, and

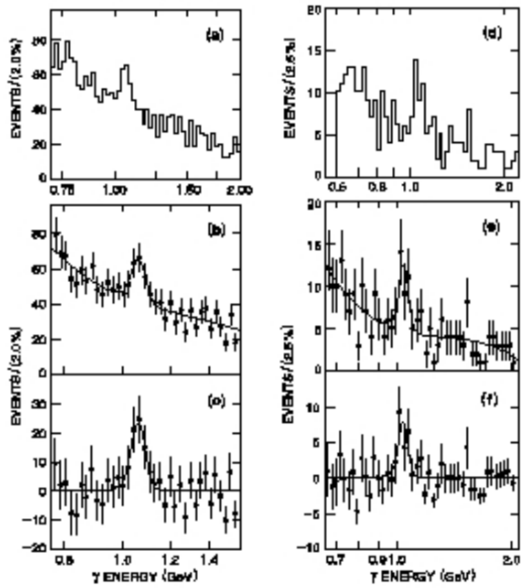

Fig. 2 Measurements from the Crystal Ball experiment in 1984, giving a preliminary indication of a resonance $\zeta(8.3)$ produced in the process $\Upsilon(1S) \to \gamma\zeta(8.3)$. The $\zeta(8.3)$ was considered by some to be a Higgs-boson candidate. The figures at left show the photon-energy spectrum in the $\zeta \to$ multi-hadrons channel (a) without the fit to the data, (b) with the fit to the data (b), and (c) after background subtraction. The figures shown at right in (d)–(f) correspond to the $\zeta \to 2$ jets channel. From Ref. [32].

$J = L + S = 1$ (in the sense of addition of angular momenta). That is, there is no relative orbital angular momentum between the b and $\bar{b}$ quarks ($L = 0$), but the two quark spins (each 1/2) are coupled in a symmetric state to a spin of $S = 1$, which is also the total spin J of the meson (since $L = 0$). The key element of the detector was an array of NaI crystals, which provided excellent photon-energy resolution. The experiment did not have a magnet, so the information on charged tracks was limited, a weakness of the measurement. Compared with the events typically observed at the LHC, those in this study had a very low particle multiplicity: the initial state consisted of a single particle, the $\Upsilon(1S)$.

The physics of $b\bar{b}$ and $c\bar{c}$ states may seem less familiar today, but the Crystal Ball experiment had a long and distinguished history at SLAC of mapping out the states in the charmonimum system by studying the spectroscopy of the radiative transitions between $c\bar{c}$ states of different quantum numbers. The detector was subsequently moved (in a U.S. Air Force transport plane) to Hamburg, where it was installed in the DORIS ring at DESY. This ring operated at a higher energy to study the Υ system as well as B mesons. The radiative decays of both $c\bar{c}$ and $b\bar{b}$ states have provided extensive information on these “onia” particles.

The Crystal Ball evidence for a state at mass of 8.3 GeV consisted of two separate photon energy spectra, each with a peak just above 1.0 GeV, as shown in Fig. 2. The two samples were separated on the basis of the characteristics of the hadronic recoil system. In the $\zeta(8.3) \to$ *multi-hadron channel*, the statistical significance was 4.2σ, while in the $\zeta(8.3) \to$ *two jets channel*, the significance was 3.3σ.

The March 1985 issue of *Physics Today* [33] contains an article entitled *Zeta revisited: Have we really seen the Higgs?* The article begins

> Much excitement was generated last summer at the XXIII International Conference on High Energy Physics in Leipzig by the Crystal Ball collaboration's report of evidence for a curious new particle, the 8.32-GeV "zeta" boson, that might well have been the long-sought-after Higgs particle.

Let's consider some of the strengths and weaknesses of the signature. A strength is certainly the narrow peak in a kinematic quantity (energy) that is reconstructed with good resolution. Furthermore, the shape of the background appears to be smooth over the width of the signal, so the sidebands can be used to estimate the background. However, the mass of the recoiling particle was not specified *a priori,* so an excess occurring in any bin in the energy range of the search could be regarded as a potential signal. The statistical implications can be quantified – this is called the *look-elsewhere effect* and is an important consideration in searches. Because the Crystal Ball did not have a powerful tracking system with a magnet, the information on the actual decay products of the $\zeta(8.3)$ was very limited. In a subsequent data sample, these signals disappeared entirely, and other experiments failed to confirm the original observation.

A second example, also from 1984, is a measurement from the UA1 experiment at the CERN Sp$\bar{\text{p}}$S collider. The paper, *Associated production of an isolated large-transverse-momentum lepton (electron or muon), and two jets at the CERN* $p\bar{p}$ *collider* [34], presented evidence for events consistent with the decay sequence $W^+ \to t\bar{b}$, $t \to b\ell^+\nu$. (Remember – this was back in the days when the top quark had not yet been discovered, and in this search it appeared that $m(t) < m(W)$! How would our searches at the LHC be affected if $W^+ \to t\bar{b}$?) The published paper includes kinematic distributions (Fig. 3) for two key mass combinations that appear to agree with this W-decay hypothesis. The invariant mass of the system consisting of the two highest energy jets, the lepton, and the neutrino is expected to peak at the mass of the W-boson. (Only the components of the neutrino momentum vector transverse to the beam axis are used, because the initial momenta of the colliding partons along the beam axis is unknown.) The invariant mass distribution of the second highest energy jet, the lepton, and the neutrino is also seen to peak at a common mass, consistent with three-body top-quark decay $t \to b\ell^+\nu$. With only six events, however, these distributions have limited power. The paper acknowledges that "that more statistics are needed to confirm these conclusions and the true nature of the effect observed." Further studies in UA1 with additional data showed that the top-quark hypothesis was not correct, and eventually the top quark was discovered at the Tevatron at a mass of around 170 GeV.

We have considered two examples of analysis problems, one from an e^+e^- experiment and one from a hadron-collider experiment. The number of signal events

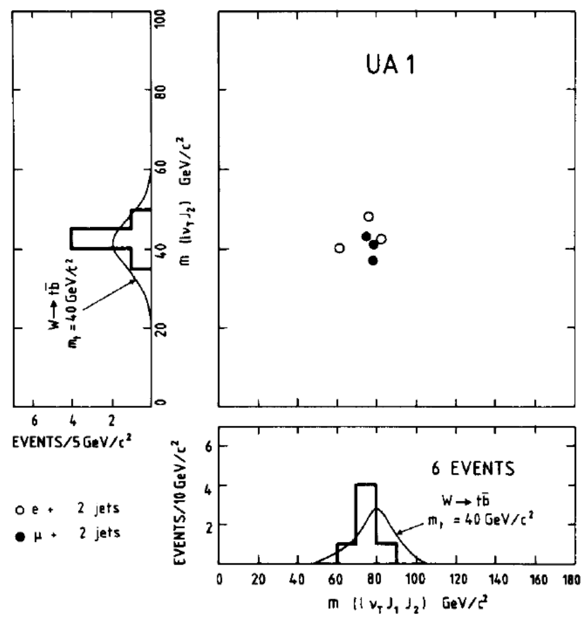

Fig. 3 UA1 experiment: kinematic distributions associated with the study of $p\bar{p}$ events with b-tagged jets, leptons, and missing transverse energy. The six events observed in data peaked both in $M(\ell\nu_T J_1 J_2)$ and in $M(\ell\nu_T J_2)$, where ν_T is the missing transverse momentum. In this study, the top quark, with mass $M_t \approx 40$ GeV, was thought to be lighter than the W boson, so the hypothetical decay sequence was $W^+ \to t\bar{b}$, $t \to b\ell^+\nu$. From Ref. [34].

was quite small in both cases, which is of course common in discovery situations. As a consequence, it can be difficult to perform meaningful cross checks on the behavior of distributions. This is particularly difficult if there is a substantial background under the signal peak. Another feature shared by these searches is that the location of the signal bin in the kinematic distribution was not *a priori* known.

The next example, the apparent observation of pentaquark states, is truly astonishing in its scope. These hypothetical particles would have valence quark content of four quarks and one anti-quark (or the conjugate). One of the several new particles apparently found was the Θ^+ pentaquark, whose quark content was assigned to be $udd u\bar{s}$, so that a natural decay mode was $\Theta^+ \to n(udd)K^+(u\bar{s})$. Note that this particle would have baryon number +1, but the $\bar{s}$ gives it the opposite strangeness of a normal baryon (such as $\Lambda \sim uds$), making it "exotic."

Figure 4 shows the reconstructed invariant-mass spectrum for the nK^+ system from the photoproduction process $\gamma d \to K^+K^-pn$ in the CLAS experiment [35]. A narrow peak was observed around 1.5 GeV with a statistical significance quoted as $(5.2 \pm 0.6)\sigma$. Remarkably, nine experiments obtained evidence for a particle around this mass, each with a significance of over 4σ and several with a significance over

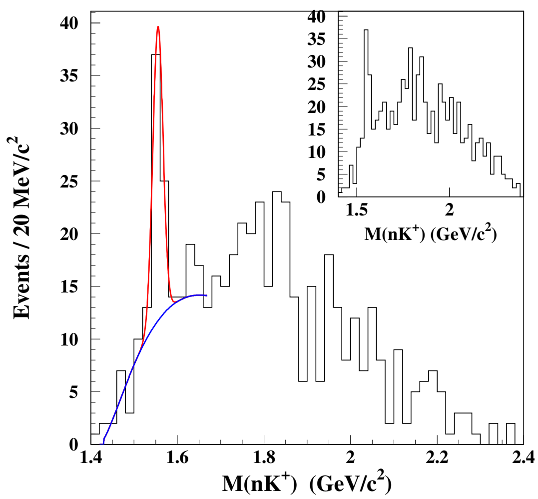

Fig. 4 CLAS experiment: study of the invariant mass distribution of the nK^+ system produced in photoproduction $\gamma d \to K^+K^-pn$. The statistical significance of the peak around 1.54 GeV was quoted to be $(5.2\pm0.6)\sigma$. From Ref. [35].

5σ [36, 37]. A perhaps telling sign of trouble was that the masses of these different observations were not entirely consistent.

This wave of discoveries, which even included a charm pentaquark, $\Theta_c^0 \to D^{(*)}p$, was followed by a wave of non-confirmations, and later on by a few additional positive sightings. The excitement that had begun around 2002 was dying down by 2005. Over 550 theoretical papers were produced during this period! An illuminating review of the various results, "The Rise and Fall of Pentaquarks in Experiments," was presented by R. Schumacher [38] at the *Particles and Fields International Conference* in 2005. His review includes a comprehensive chronology of observations and non-observations of pentaquark states. He concludes that

> Thus, one can conclude that a "bandwagon" rush of over-optimistic positive sightings was in effect initially, but now the lack of convincing evidence for narrow exotic pentaquarks is overwhelming.

For many of the pentaquark searches the underlying physics of the background processes (and hence the background shapes) was not well understood. In this context, the true statistical significance of peaks can be very difficult to assess [37].

4.2 Lessons Learned: Common Problems in Searches for New Physics

What lessons can we learn from these (and many other) examples in our field? First of all, searches are difficult! Here is a list of some common mistakes or situations that occur. Do any of these affect your analysis?

- The detector may not be correctly calibrated or aligned, leading to mismeasured objects in events.
- Limitations in the detector design or technology can produce spectacular mismeasurements such as E_T^{miss} or lepton isolation in rare circumstances. Event displays can be useful for identifying unusual problems, but they can also be used in a problematic way to reject events without a well-defined procedure.
- Trigger efficiencies (including their kinematic dependence) may not be fully accounted for and can bias yields in the signal or control regions.
- Changes in the experimental conditions or calibrations may not be fully taken into account. For example, at the LHC, the presence of multiple pp collisions within a single beam crossing leads to multiple vertices and can affect many reconstructed quantities. This effect is luminosity dependent.
- A prescription for a "standard" analysis method or reconstructed object (b-tagged jets, leptons, etc.) may not give the correct result when applied in the sample of events used in your analysis. Was the standard recipe validated in an event sample in which the relevant properties are similar to yours?
- Monte Carlo event samples may not have been generated correctly.
- Monte Carlo event samples may not have correctly modeled the true physics. For example, the number of extra jets from initial- or final-state radiation may not be correct. The simulation may not model all of the kinematic correlations in the signal, leading to an incorrectly estimated signal efficiency.
- The yield in signal region can be biased by tuning selection requirements on the signal region in the data.
- The yield in the signal region can be biased by tuning selection requirements on the region used to determine the background to be subtracted.
- The background shape or normalization may be estimated incorrectly. Background estimates are especially tricky if there are contributions from many sources or if control samples are obtained with different triggers.
- Understanding the background in one kinematic region does not necessarily mean that you understand it in another region. The background composition may vary substantially from a control sample to a signal region, and the kinematic distributions may also vary between these regions.
- The shapes used in a fit may not be adequate to describe the data, which can easily produce a bias in the extracted signal yield. This effect is especially worrisome in multidimensional fits, where the shapes may not fully track the correlations among kinematic variables.
- Theoretical assumptions used to determine the backgrounds or their uncertainties may be incorrect. Consultation with theorists can be valuable in such cases.

- Systematic uncertainties may be underestimated or incomplete.
- Correlations may not be taken into account correctly. Correlations can arise from many different mechanisms. Two kinematic quantities can become correlated not only analytically, within a given sample of events, but also through a variation in the sample composition as one variable is changed.
- Backgrounds peaking under the signal may not be fully taken into account.
- The signal efficiency may be incorrectly determined.
- The signal significance may not be be estimated correctly.
- The look-elsewhere effect may not have been taken into account in assessing the statistical significance.
- A signal can be created artificially as a “reflection” of a background process that produces a peak or other structure in a related kinematic variable.
- Averaging multiple measurements can be tricky; all uncertainties and their correlations must be understood.
- Bug in your program. Bug in someone else’s program. Bug in ROOT.
- Advisor is in a hurry! Need to finish thesis! No time to look for more problems!
- People sometimes stop looking for mistakes or declare a result ready to be presented publically when they obtain a “desirable” result. In precision measurements, people sometimes prefer to obtain agreement with previous results, leading to a clustering of measurements that is better than the uncertainties should typically allow.
- A superposition of several of the above effects.

How many of these have you actually seen in practice? Based on conversations with students at this school, I conclude that graduate students are quite familiar with these problems, as well as many others not listed. A fundamental problem, which may simply be a statement about entropy, is that there are many ways to do something wrong, but far fewer ways to do things right! One approach, blind analysis [39, 40], offers some valuable methods but also some potential problems, especially when the event sample has not previously been explored. In general, it is important to design your analysis with as many crosschecks and control sample studies as you can to provide comprehensive tests of the analysis methods.

5 Characteristics of Standard Model Backgrounds

Before discussing specific searches for new physics, we consider in Section 5.1 the main SM processes that typically contribute to the backgrounds. Section 5.2 focuses on the properties of $t\bar{t}$ events, which are the dominant source of background in many new physics searches.

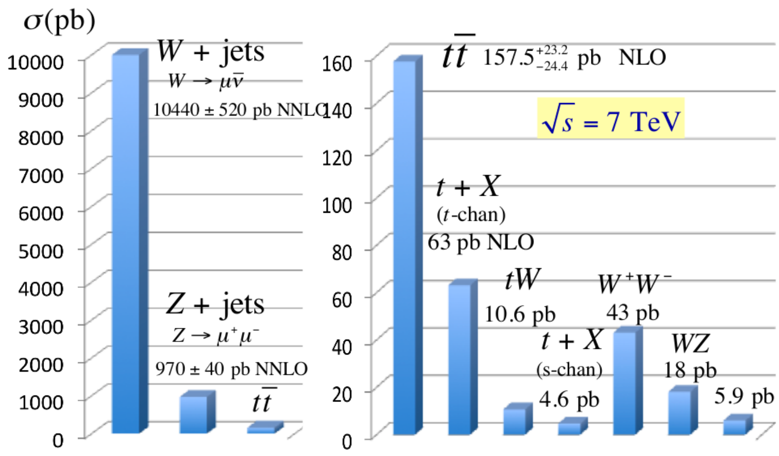

Fig. 5 Cross sections at $\sqrt{s} = 7$ TeV for common SM processes relevant to searches. Note the change in scale between the left- and right-hand parts of the figure. The cross sections for W and Z production include the branching fractions for the leptonic decay modes specified.

5.1 Survey of SM Backgrounds and Their Role in New Physics Searches

Detailed studies of SM background processes are valuable and often essential for searches. As the LHC luminosity increases, and we search for new physics with lower cross sections, the number of relevant SM background processes is increasing. These processes are interesting in their own right. If you are studying a SM process, you are contributing to the searches for new physics as well.

People sometimes believe that it is "conservative" to overestimate the background, because one is then less likely to claim a false signal. Overestimating the background is not a good practice, however. First of all, if a signal is present, you want to know it, not hide it! But even if no excess is observed, and you are setting an upper limit, subtracting an overestimated background from the yield in the signal region leads to its own problems. You will then underestimate the number of events in the signal region that can potentially be attributed to signal, and your limit will be more stringent than it deserves to be. It is not conservative to overestimate the background!

Figure 5 shows some of the key cross sections for W+jets, Z+jets, $t\bar{t}$, single-top, and diboson production processes. The cross sections for W and Z production include the branching fractions for $W \to \mu\bar{\nu}$ and $Z \to \mu^+\mu^-$, respectively. The separate production cross sections for W^+ and W^- are not shown, but these are

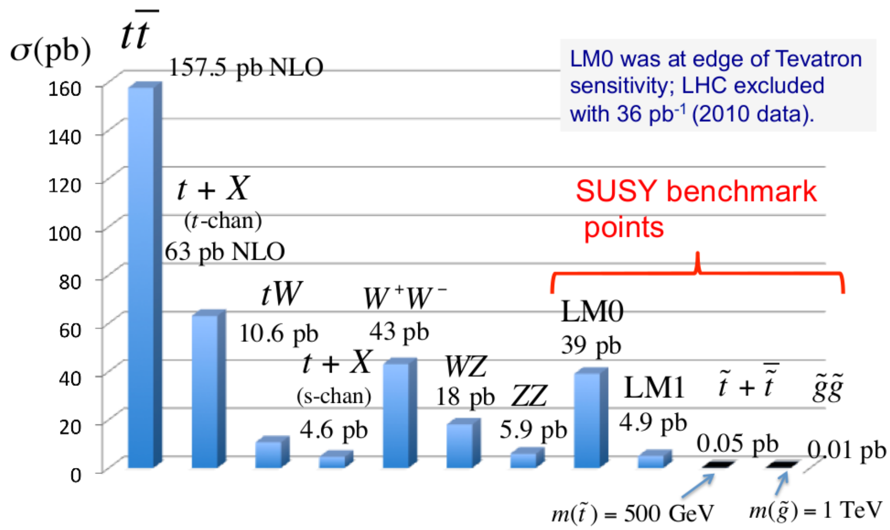

Fig. 6 Cross sections at $\sqrt{s} = 7$ TeV for processes involving top quark production and diboson production, as well as for some benchmark SUSY models.

different (as are their kinematic distributions), reflecting the charge asymmetry of the pp initial state.

Although they are not shown, the cross sections for QCD multijet processes are very large and depend strongly on the jet p_T thresholds that are applied. In fact, these cross sections are so large that it is often impossible to generate a sufficient number of Monte Carlo events to study their contribution to an LHC data sample. Although QCD multijet events can often be suppressed to a level well below that of the other backgrounds, the residual contribution must still be quantified with reliable uncertainties. Because the accuracy of QCD simulations is questionable, Monte Carlo samples are best used to gain insight into the behavior of the backgrounds rather than to determine any quantitative result. In general, QCD multijet backgrounds should be determined using control samples in the data.

Figure 6 focuses on the SM process with smaller cross sections and adds a few SUSY models for comparison. Models LM0 and LM1 are low-mass SUSY models [41] that were used in early CMS searches. They are defined in the framework of the constrained minimal supersymmetric standard model [11] (cMSSM, closely related to minimal supergravity, or mSUGRA). LM0 was defined as a reference near the edge of Tevatron sensitivity and was quickly excluded in the first LHC run. The cross sections for gluino pair production and stop (scalar top) production are also shown for certain mass parameters. These cross sections are strong functions of the SUSY particle masses and will be discussed later.

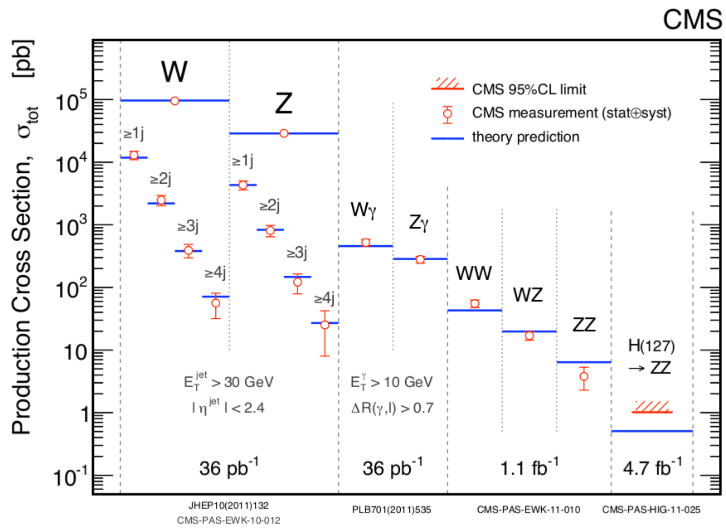

Fig. 7 Measured (CMS) and theoretical cross sections for processes involving W and Z bosons ($\sqrt{s} = 7$ TeV). The cross sections fall off exponentially as the number of jets increases. The jet transverse-energy thresholds are specified in the figure.

The cross sections for processes involving the production of W and Z bosons are shown in more detail in Figure 7. The W and Z cross sections are given as a function of the number of recoiling jets.

What general observations can we make regarding the behavior of backgrounds in different search channels? Here are a few:

- Backgrounds from W+jets and Z+jets events fall off rapidly as the number of jets increases. For signatures with large numbers of jets, this effect often suppresses these backgrounds below that from $t\bar{t}$ production.
- In searches that require large missing transverse energy (E_T^{miss}), backgrounds from $W \to \ell\bar{\nu}$, $Z \to \nu\bar{\nu}$, and $t\bar{t}$ events with $W \to \ell\bar{\nu}$ typically play a major role. The large E_T^{miss} in such events is genuine, associated with high-momentum neutrinos from W or Z decay. However, mismeasured jets (sometimes associated with detector problems) or jets containing a neutrino from semileptonic b-quark decay can also lead to large E_T^{miss}. *Thus, a large value of E_T^{miss} does not necessarily indicate the presence of a weakly interacting particle produced in the initial hard scattering or in the decay of heavy particles.*
- In searches for signatures with large E_T^{miss} and no leptons, $(Z \to \nu\bar{\nu})$+jets represents an "irreducible" background, with the same topology as the signal. However, SM processes in which the lepton from W decay is missed can also be substantial. Such missed leptons arise not only from detector inefficiencies, but also from leptons that fail to satisfy lepton p_T and isolation requirements. An-

other important source of events with E_T^{miss} arises from τ-lepton decays, either to lighter charged leptons or final states with hadrons, such as $\tau^- \to \pi^- \nu$.

- In searches that include jets, E_T^{miss}, and a single isolated lepton in the signature, backgrounds arise mainly from $t\bar{t}$ and $W \to \ell\bar{\nu}$. By requiring $M_T(\ell\bar{\nu}) > 100$ GeV (where the ν is inferred from E_T^{miss}), backgrounds with a single W boson can be strongly suppressed, so that contributions from $t\bar{t}$ dilepton events become dominant.
- In searches that include two opposite-sign isolated leptons in the signature, $t\bar{t}$ is a critical background. If the signature involves same-flavour leptons only, the unlike-flavour sample in the data can, with care, be used to measure the contribution from $t\bar{t}$ events.
- Searches for signatures with like-sign leptons are special, in the sense that these are highly suppressed in SM processes. In $t\bar{t}$ events, a primary lepton (from W decay) and a secondary lepton (from b decay) can produce like-sign lepton background, but this contribution can be strongly suppressed with a lepton isolation requirement.
- QCD backgrounds are strongly suppressed by requiring either an isolated lepton or large E_T^{miss}. In addition, the E_T^{miss} in such events is usually aligned with one of the jets. However, the QCD cross sections are so large that one must determine whether unusual event configurations are contributing to the signal region. Such events can arise from detector mismeasurements, producing fake E_T^{miss}, or semileptonic decays of b- and c-hadrons in jets.
- Lepton isolation is a critical variable for determining whether leptons are produced in the decay of a heavy particle. However, isolation does not provide a perfect separation of such primary leptons from secondary leptons.
- In searches with one or more high-transverse-energy photons, the isolation of the photon plays a critical role, similar to that for leptons.
- A requirement of multiple b jets, which is applied in many searches for processes with $\tilde{t}$ or $\tilde{b}$ squarks, helps to suppress W+jets and Z+jets backgrounds. This behavior is another reason why $t\bar{t}$ is such an important background process.
- New physics processes with rates comparable to those from these SM common processes are now largely excluded. As a consequence, searches for new physics typically require a careful understanding of the *tails* of the kinematic distributions of SM processes. As the luminosity increases, additional rare SM processes will become relevant.

Methods for determining background contributions range from simple to highly involved. Regardless of the method, it is always important to understand the background composition and to explore how it varies as the selection criteria are applied. Simulated event samples are extremely useful for this purpose. If the signal is a sufficiently narrow peak over a slowly varying background, the background is usually estimated from a fit the effectively extrapolates the sidebands into the signal region. In many searches, including nearly all searches for SUSY, the signal is simply an excess of events in the tail of a distribution such as E_T^{miss}. In this case, much more effort and care is required to obtain a reliable background prediction.

In the simplest approach, simulated events samples are generated, reconstructed, and analyzed using procedures that are as close as possible to those used for the data. Typically, corrections must also be applied to account for known differences between the actual detector and the simulated detector. Because the trigger conditions typically vary over the data-taking period (for example, as the luminosity increases), it is difficult to model them correctly in simulated event samples. To simplify the determination of the trigger efficiency, one typically applies an offline selection requirement that is somewhat more stringent than the most stringent trigger requirement, establishing a uniform condition over the full running period. It is also common practice to set the offline requirement such that the trigger efficiency is on the plateau with respect to the applied thresholds.

The use of simulation for predicting backgrounds has several potential problems, which are widely recognized. Because searches for new physics processes typically involve event-selection requirements that strongly suppress SM backgrounds, the amount of residual background often depends on the how the backgrounds behave in a narrow region of phase space. The modeling of the so-called tails of the kinematic distributions may not be as accurate as the modeling of the cores, where most of the events are, and where the simulation is often validated most fully with control samples. In addition, some types of detector problems may not be modeled in simulated event samples. It is not unusual to see the quantitative agreement between data and simulation worsen significantly as the analysis cuts are applied.

In practice, one rarely sees an analysis in which the key background estimates are obtained simply by taking the yields from simulation, normalized to the integrated luminosity of the data sample. A more common practice is to normalize a distribution from simulation either in a sideband region that should be relatively free of signal (for the model considered!) or in a control region obtained by altering one or more of the cuts. This procedure has some virtues, especially that the burden on simulation is much reduced. However, it is not entirely free of potential problems; for example, the composition of the control sample may not be fully understood. It can also be difficult to reliably quantify the uncertainty on the scale factors required to translate the observed background yield in the control region to the observed background yield in the signal region.

The term *data-driven background prediction* is used to describe any method that relies largely on control samples in the data to estimate the background. An example is the use of a photon + jets control sample to predict the background from $Z \to \nu\bar{\nu}$+jets events, a highly non-trivial exercise. The best data-driven methods rely on specific, well-understood properties of SM processes for which the uncertainties can be quantified in a well-defined manner.

5.2 Discussion of a Key SM Background: $pp \to t\bar{t}$

Many searches involve high-mass objects, which have complicated decay chains and signatures containing a large number of jets and other objects. (A notable ex-

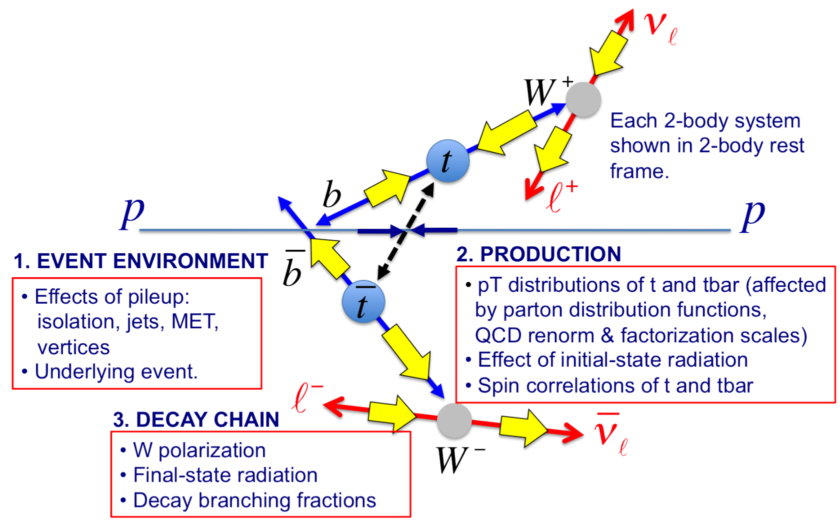

Fig. 8 An overview of key issues in understanding $t\bar{t}$ production in pp collisions: event environment, production, and decay chain.

ception is the search for new heavy gauge bosons using the signatures $Z' \to \ell^+\ell^-$ and $W'^- \to \ell^-\bar{\nu}$.) Because of the large top-quark mass, SM $t\bar{t}$ production is a prototypical background, leading to events with high jet multiplicity, isolated leptons, and $E_T^{\rm miss}$.

Figure 8 summarizes the key experimental issues that arise in $t\bar{t}$ events. These can be divided into three (somewhat arbitrarily defined) categories: (1) the event environment, (2) the production properties, and (3) the decay chains. The *event environment* encompasses such features as multiple pp collisions and the properties of the underlying event (the particles that are not produced in the hard scattering processes). *Production* effects include the p_T distribution of the top quarks. These are affected strongly by the parton distribution functions, of course, but the p_T distributions are more directly relevant to measurements. The extent of the tails of the p_T distributions can be particularly important for searches involving $E_T^{\rm miss}$, because $t\bar{t}$ events with the very highest $E_T^{\rm miss}$ values usually arise when neutrinos from $t \to bW^+$, $W^+ \to \ell^+\bar{\nu}$ are Lorentz boosted to high energy in the laboratory frame. The production of additional jets from initial- and final-state radiation can be an important issue for analyses in which jet multiplicity plays a key role. For example, a SUSY search in the dilepton final state might well require the presence of at least three jets to suppress background from $t\bar{t}$ in which both W bosons decay leptonically. The decay chains produce only two (b) jets, one each from $t \to bW$, but QCD radiation can produce additional jets. Finally, the *decay chain* itself involves effects such as the W-boson spin polarization, which controls the angular distribution of the W-boson decay products and hence their momenta in the laboratory frame.

As an example of one of these issues, let's consider the W-boson spin polarization in top-quark decay and its effect on the decay $W^+ \to \ell^+\nu$, where ℓ^+ is any charged lepton. This sequential two-body decay process is well understood in the SM, and it has been studied experimentally, although interesting new physics effects could in principle enter at a low level. As discussed below, the effects of QCD on the W-boson polarization have been calculated to NNLO; these corrections are small with respect to the basic, weak-interaction behavior. Here are some questions to think about:

1. In the top-quark rest frame, which distribution is harder, the momentum spectrum of the charged lepton or the neutrino?
2. Is the polarization of the W boson the same in t and $\bar{t}$ decay? Hint: no, but they are directly related.
3. Are the kinematic distributions of the lepton and neutrino the same for t and $\bar{t}$ decay? Hint: yes (fortunately).

Figure 9 shows three spin configurations for the decay of a top quark. We begin with the top quark, which is shown in the laboratory frame in a helicy $\lambda = -1/2$ state, indicated by a fat yellow arrow pointing in the direction opposite to its momentum vector. This does not mean that top quarks can only be produced with this helicity; in fact, in strong production there is no preference for either helicity. (There are, however, correlations between the helicities of the two top quarks, which can generate small but noticable effects in a dilepton analysis.) The figure also shows the decay $t \to bW^+$, illustrated with back-to-back momentum vectors for the b-quark and the W^+ boson. *These momentum vectors are shown in the t-quark rest frame.* Thus, the drawing shows two *different* reference frames, the lab frame and the t-quark rest frame. This convention is commonly used because it breaks the analysis of the decays into two parts: (1) angular distributions in the rest frame of the decaying particle and (2) Lorentz boosts to the frame in which the decaying particle is observed.

Top-quark decay is controlled by a $V-A$ coupling at the tW^+b vertex, which couples only to the left-handed chiral projection of the b quark. *In the relativistic limit,* this left-handed chiral projection maps onto the helicity $\lambda(b) = -1/2$ component of the b-quark. Because $m_b << m_t$, the b-quark is in fact relativistic, so the amplitude for helicity $\lambda(b) = -1/2$ completely dominates, and in each of these three cases shown in Fig. 9, the b-quark is shown with this helicity.

The decay configuration on the left, however, is forbidden by conservation of angular momentum. Because the momenta of the b-quark and the W^+ boson are aligned in the t-quark rest frame, we can sum all of the angular momenta along this axis. For the configuration with $\lambda(W^+) = +1$ and $\lambda(b) = -1/2$, the magnitude of the total angular momentum along the decay axis must be $3/2$. This spin projection would be greater than the spin of the top quark (1/2), so it cannot possibly conserve angular momentum. Note that *there cannot be any orbital angular momentum projection along a two-body decay axis*, because $\mathbf{L} = \mathbf{r} \times \mathbf{p}$. Any *orbital* angular momentum must be *perpendicular* to this axis! Thus, to a very good approximation, there are only two allowed helicities for the W^+ boson: $\lambda(W^+) = 0$, which

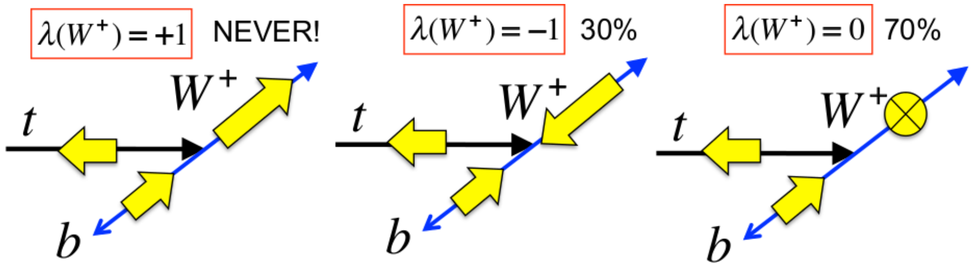

Fig. 9 Examples of spin configurations in top-quark decay. The top quark is shown (arbitarily) in the helicity state $\lambda(t) = -1/2$; this is not important for the discussion. Because of the $V-A$ coupling at the decay vertex, the daughter b-quark, which is relativistic, is predominantly in the state $\lambda(b) = -1/2$. The W^+ boson cannot then be in the state $\lambda(W) = +1$ because this would yield an angular momentum projection along the decay axis of $3/2$, which is greater than the spin of the t quark.

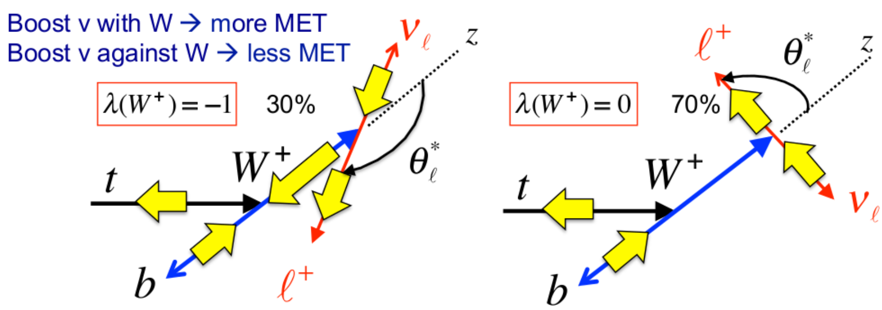

Fig. 10 The sequential two-body decay process $t \to bW^+$, $W^+ \to \mu^+\bar{\nu}$. *Each two-body decay is shown in its respective rest frame.* For the case $\lambda(W^+) = -1$ the lepton is emitted preferentially in the backward direction in the W^+ rest frame. The neutrino is correspondingly emitted preferentially in the forward direction, creating an asymmetry between the lepton p_T and E_T^{miss} distributions in the t-quark rest frame and in the laboratory frame.

it turns out occurs about 70% of the time, and $\lambda(W^+) = -1$, which occurs 30% of the time. There is a tiny amplitude for $\lambda(W^+) = +1$ and $\lambda(b) = +1/2$, which is present because the b quark is not massless. These probabilities are reliable SM predictions and are calculated to be $f_0 = 0.687 \pm 0.005$, $f_{-1} = 0.311 \pm 0.005$, and $f_{+1} = 0.0017 \pm 0.0001$ [42] at NNLO in QCD.

We turn now to the decay of the W^+ boson into $\ell^+\nu$, where the W boson is produced in top-quark decay (Figure 10). For the case $\lambda(W^+) = -1$, the lepton is emitted preferentially in the backward direction, with a distribution given by $dN/d\cos\theta_{\ell^*} \sim (1-\cos\theta^*_\ell)^2$. This result uses conservation of angular momentum, which implies that in any two-body decay $A(J,M) \to B(\lambda_B) + C(\lambda_C)$, the distribution of the polar angle θ of particle B with respect to the z axis is given by [43, 44]

$$dN/d\cos\theta \sim [d^J_{M,\lambda(B)-\lambda(C)}(\theta)]^2. \quad (3)$$

Here, J is the spin of the parent particle A and M is its spin projection along the z axis; $\lambda(B)$ is the helicity of particle B; and $\lambda(C)$ is the helicity of particle C. Thus, for $\lambda(W^+) = -1$, the neutrino is emitted in the forward direction with respect to the momentum of the W^+ as observed in the t-quark rest frame; it is therefore boosted to higher energy in that frame. For $\lambda(W^+) = 0$, the lepton angular distribution is symmetric in θ^*_ℓ: $dN/d\cos\theta^*_\ell \sim \sin^2\theta^*_\ell$. For this W polarization, the distributions of the lepton and neutrino momentum in the top-quark rest frame are the same.

The helicities of the W, lepton, and neutrino all reverse when we switch from t to $\bar{t}$ decay, leading to the result that the angular distributions for the lepton are the same in t and $\bar{t}$ decay chains. (The probability for $\lambda(W^-) = +1$ is $\approx 30\%$ in $\bar{t} \to \bar{b}W^-$ decay, corresponding to the probability for $\lambda(W^+) = -1$ in $t \to bW^+$ decay.) Thus, for both t and $\bar{t}$ decay, the neutrino (E_T^{miss}) distribution is harder than that of the lepton p_T distribution in the laboratory frame. The relationship between the lepton spectrum and the E_T^{miss} spectrum in $t\bar{t}$ events has been used as the basis for data-driven background predictions in a number of SUSY searches [45, 46].

Other examples of phenomenology papers that provide important information on SM processes relevant to new physics searches are the predictions for W-boson polarization fractions in W + jets events [47] and predictions for $\gamma+$ jets events and their relationship to $Z+$ jets events [48].

6 Searches for Supersymmetry at the LHC

Supersymmetry (SUSY) is a general framework that encompasses many different theories or models, which are associated with the specific mechanisms that break the symmetry. Each of these models can have a broad range of parameter values. Thus, the most generic approach to SUSY leads to many distinct phenomenological situations, presenting challenges for both experiment and theory. An issue of special importance is defining the set of criteria used to trigger the readout of the detector. There are interesting models for which, without special care, the detector would not even trigger on SUSY events. The large number of models also creates a challenge in *interpreting* the results of a given search, because exclusion plots for one model often cannot be translated into limits for a different model.

Theorists have developed models in which the number of parameters is reduced by applying various constraints. For example, the constrained Minimal Supersymmetric Standard Model (cMSSM) [11, 49, 50] has just four continuous real parameters and a sign, but many theorists do not consider its underlying assumptions to be especially well motivated. A more generic approach is the phenomenological minimal supersymmetric standard model (pMSSM) [51, 52], which incorporates a number of phenomenological constraints and has 19 real parameters beyond those of the SM. Another recent theoretical strategy, exemplified by *simplified models* [53, 54, 55, 56], has been to focus on distinct phenomenological signatures that can be interpreted in more than one theory. In Section 6.1 we begin with a basic introduction to SUSY phenomenology. Section 6.2 describes the methods used in some of the important searches and summarizes their results.

6.1 A First Look at SUSY Phenomenology

SUSY is based on a mapping between fermionic and bosonic degrees of freedom. A SM spin-1/2 particle, such as the electron, has two spin states, so that two matching bosonic degrees of freedom are required. When a SUSY transformation is performed on a SM field, the transformed field has the same gauge quantum numbers as the original field: each of the $SU(3)_C \times SU(2)_L \times U(1)_Y$ quantum numbers is exactly preserved. For example, when a SUSY transformation acts on a gluon field, yielding a gluino field, the gluino has exactly the same colour quantum numbers as the gluon and hence transforms under $SU(3)_C$ rotations in the same way, according to the adjoint representation.

Returning to leptons, the $SU(2)_L$ quantum numbers of the electron are different for the left- and right-handed chiral projections. The e_L is part of an $SU(2)_L$ weak-isospin doublet together with the electron neutrino, ν_e. The e_R, in contrast, transforms as a singlet under $SU(2)_L$ rotations: it has zero weak isospin and does not couple to the W boson. Because SUSY preserves these quantum numbers, each of these chiral projections is a degree of freedom of the electron that maps onto its own scalar electron, or selectron. These scalar partners are designated as $\tilde{e}_L$ and $\tilde{e}_R$, even though they themselves are spinless. The subscripts mean that the selectrons are the *partners* of the left- and right-handed electrons; furthermore, they have the corresponding L and R electroweak gauge quantum numbers. Similarly, the L- and R-handed chiral components of each quark map separately onto two scalar quarks (squarks), $\tilde{q}_L$ and $\tilde{q}_R$. In general, the SUSY partners $\tilde{f}_L$ and $\tilde{f}_R$ of an SM fermion f have different masses after SUSY breaking.

In the minimal supersymmetric standard model (MSSM), the Higgs sector requires two complex doublet fields, not just the one we are familiar with in the SM. (The MSSM is discussed extensively at this school by Sven Heinemeyer.) Altogether, the MSSM has 124 free parameters, including the 18 parameters of the SM embedded within it. We have already discussed how the fermion fields in the SM (associated with leptons and quarks) map onto scalar fields (associated with sleptons and squarks), and how the gluon field maps onto the gluino field. This leaves the electroweak gauge bosons and the Higgs bosons.

Figure 11 lists the particles that make up the electroweak gauge and Higgs sectors of the MSSM. The left-hand table lists the gauge and Higgs bosons, while the middle table lists their fermionic SUSY partners, the gauginos and higgsinos. In each case, there are a total of 16 degrees of freedom. In general, mixing effects among the neutral gauginos and neutral higgsinos lead to the set of physical particles (mass eigenstates), the neutralinos, which are designated by the symbol $\tilde{\chi}_i^0$. Similarly, mixing effects among the charged gauginos and charged higginos lead to

Particle	J	Degrees of freedom
W^+	1	3
W^-	1	3
Z	1	3
γ	1	2
H	0	1
h	0	1
H^+	0	1
H^-	0	1
A	0	1
Total		16

Particle	J	Degrees of freedom
$\tilde{W}^+$	1/2	2
$\tilde{W}^-$	1/2	2
$\tilde{Z}$ / $\tilde{W}^0$	1/2	2
$\tilde{\gamma}$ / $\tilde{B}$	1/2	2
$\tilde{H}$	1/2	2
$\tilde{h}$	1/2	2
$\tilde{H}^+$	1/2	2
$\tilde{H}^-$	1/2	2
Total		16

Mixing

Particle	J	Degrees of freedom
$\tilde{\chi}_1^+$	1/2	2
$\tilde{\chi}_1^-$	1/2	2
$\tilde{\chi}_2^+$	1/2	2
$\tilde{\chi}_2^-$	1/2	2
$\tilde{\chi}_1^0$	1/2	2
$\tilde{\chi}_2^0$	1/2	2
$\tilde{\chi}_3^0$	1/2	2
$\tilde{\chi}_4^0$	1/2	2
Total		16

Fig. 11 The gauge and Higgs sectors of the Minimal Supersymmetric Standard Model (MSSM). The table on the left lists the gauge and Higgs bosons of the MSSM, which together have 16 degrees of freedom. The MSSM requires two complex Higgs doublets, not just one, as in the case of the SM. The SUSY partners, gauginos and higgsinos, are listed in the middle table. Mixing among the neutral gauginos and higgsinos leads to mass eigenstates called neutralinos; mixing among the charged gauginos and higgsinos leads to mass eignenstates called charginos, shown in the right-hand table.

physical particles called charginos, $\tilde{\chi}_i^{\pm}$. These particles are listed in the table at the right of Fig. 11. There are four neutralinos ($\tilde{\chi}_1^0$, $\tilde{\chi}_2^0$, $\tilde{\chi}_3^0$, $\tilde{\chi}_4^0$), numbered in order of increasing mass. There are four charginos, $\tilde{\chi}_1^{\pm}$ and $\tilde{\chi}_2^{\pm}$. Each of these "-ino" particles has spin-1/2. As before, there are 16 degrees of freedom. Both the gluinos and the neutralinos are Majorana fermions. If you think it is crazy to more or less double the number of particles, consider the prediction of antimatter!

SUSY, if it exists, must be a broken symmetry because partners with masses equal to those of the SM particles would already have been discovered. (This fact does not compromise the SUSY solution to the gauge-hierarchy problem as long as the SUSY breaking mechanism is *soft*, as discussed in Ref. [11].) SUSY breaking is a complex subject with various scenarios; this phenomenon occurs in a so-called *hidden sector* of particles that have no tree-level interactions with the *visible sector* (e.g., the MSSM spectrum discussed earlier). The breaking of SUSY is then transmitted from the hidden to the visible sector through some mediation mechanism, which can be a set of additional particles constituting a *messenger sector.* The proposed mechanisms include gravity-mediated SUSY breaking [11, 57], leading to a heavy gravitino ($\tilde{G}$), and gauge mediation, leading to a very light gravitino, with mass typically in the eV range. In models with gauge mediation [58, 59, 60, 61, 62, 63, 64, 65, 66] the next-to-lightest SUSY particle (NLSP) can decay into its superpartner plus a gravitino, for example, $\tilde{\chi}^0 \to \gamma\tilde{G}$, $\tilde{\chi}^0 \to Z\tilde{G}$, or $\tilde{\tau}_R^{\pm} \to \tau^{\pm}\tilde{G}$. Whatever the SUSY breaking mechanism, SUSY particles still have the same SM gauge properties as their ordinary SM partners. This is a key point when thinking about the phenomenology of the decay modes. Your intuition from the SM will serve you surprisingly well!

The MSSM possesses $B-L$ symmetry, which leads to a multiplicatively conserved quantum number called R-parity [67],

$$R = (-1)^{3(B-L)+2S}, \tag{4}$$

where B is the baryon number, L the lepton number, and S the spin of the particle. You can verify that for all ordinary SM particles $R = 1$, while for all the SUSY partners $R = -1$. A valid fundamental vertex of the SM can be converted into a valid fundamental vertex involving SUSY particles by replacing an even number of SM particles with their SUSY partners. Conservation of R-parity has major consequences:

1. Starting from an initial state containing only SM particles, SUSY particles must be produced in pairs.
2. The decay chain of a SUSY particle must end with the production of the lightest supersymmetric particle (LSP), which is stable, and which in many scenarios is $\tilde{\chi}_1^0$. Because it is stable and only weakly interacting, the $\tilde{\chi}_1^0$ LSP is a potential dark-matter candidate. Events in such models are typically characterized by large E_T^{miss} resulting from the presence of two such SUSY decay chains, each ending with a $\tilde{\chi}_1^0$.

Searches for models without R-parity conservation cannot rely on the E_T^{miss} signature and are typically quite different in their strategy.

Figure 12 shows the mass spectrum of the model LM6, which has been used as a benchmark by CMS but is now in the excluded part of the cMSSM parameter space. In this model, the gluino is the heaviest SUSY particle, while $\tilde{\chi}_1^0$, the lightest neutralino, is the LSP. In the case of the stop ($\tilde{t}$), large mixing can arise between the L- and R-handed SUSY partners ($\tilde{t}_L$ and $\tilde{t}_R$), resulting in a large mass splitting between the mass eigenstates. (See, for example, Ref. [13].) These particles are labeled $\tilde{t}_1$ (lighter) and $\tilde{t}_2$ (heavier). From Fig. 12 it is clear that in the LM6 model, $\tilde{t}_1$ is substantially lighter than all of the other squarks, followed by $\tilde{b}_1$.

The phenomenology of a given SUSY model can often be understood in a reasonably straightforward way from the mass spectrum and mixing parameters, together with the usual gauge couplings. The two key issues for experimental searches are the production cross sections and the decay branching fractions. We consider these in general and then return to the example of LM6.

The production cross sections for SUSY particles at $\sqrt{s} = 8$ TeV as a function of their masses are shown in Fig. 13. The particles fall into two broad categories: those with colour charge (squarks and gluinos), which can be produced via the strong interactions, and those that have only have electroweak couplings: the sleptons, sneutrinos, charginos, and neutralinos. The large cross sections for strongly produced particles represent a big advantage for searches, but some of the particles produced via electroweak processes can produce very distinctive signatures, making the searches quite feasible, even at very low cross sections. In this plot, the

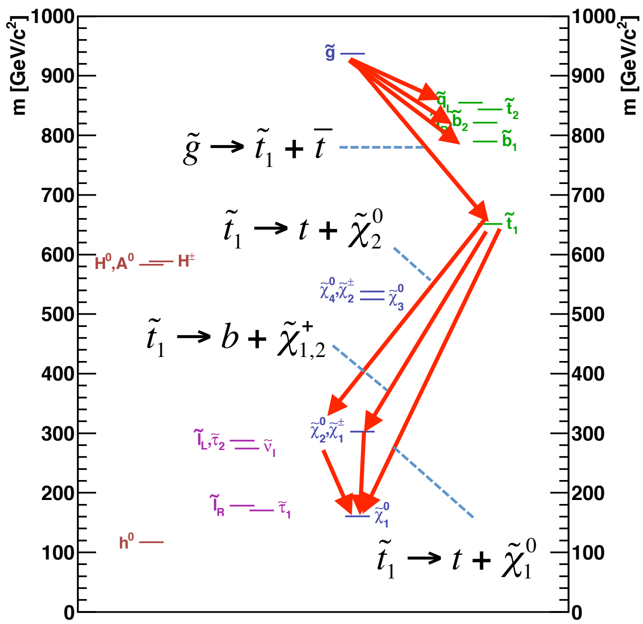

Fig. 12 Mass spectrum for the benchmark model LM6, with some of the possible decay modes indicated. These correspond to the processes $\tilde{g} \rightarrow \tilde{t}_1\bar{t}$, $\tilde{t}_1 \rightarrow t\tilde{\chi}^0_{1,2}$, and $\tilde{t}_1 \rightarrow b\tilde{\chi}^+_{1,2}$. In pp collisions, any of the SUSY particles can be produced directly, although particles with colour charge typically have larger cross sections.

symbol $\tilde{q}$ represents the sum over $\tilde{u}$, $\tilde{d}$, $\tilde{c}$, $\tilde{s}$, and $\tilde{b}$, with both L- and R-handed partners included. The cross section for production of $\tilde{t}_1\bar{\tilde{t}}_1$ is much less than that for $\tilde{g}\tilde{g}$ at the same mass (and is also much smaller than that for $t\bar{t}$, as discussed in Sec. 6.2). SUSY particle production at the LHC, including uncertainties from parton distribution functions and other sources, is discussed in the references [68, 69, 70].

Figure 14 shows the diagrams for processes contributing to gluino pair production in a SUSY model with R-parity conservation. The decay of a gluino proceeds in analogy to the SM process $g \rightarrow q\bar{q}$, governed by the same strong coupling constant. In an R-parity conserving model there are four possible decay modes for each quark flavour:

$$\tilde{g} \rightarrow q + \bar{\tilde{q}}_L, \qquad \bar{q} + \tilde{q}_L, \qquad q + \bar{\tilde{q}}_R, \qquad \bar{q} + \tilde{q}_R. \tag{5}$$

Two cases arise:

1. $m(\tilde{g}) > m(\tilde{q}) + m(q)$: true two-body decay
2. $m(\tilde{g}) < m(\tilde{q}) + m(q)$: the squark is virtual (three-body decay)

The subscripts L, R (or $1, 2$) have been omitted for generality. In the case of three-body decay, an example of a decay chain with a virtual $\tilde{b}$ squark is

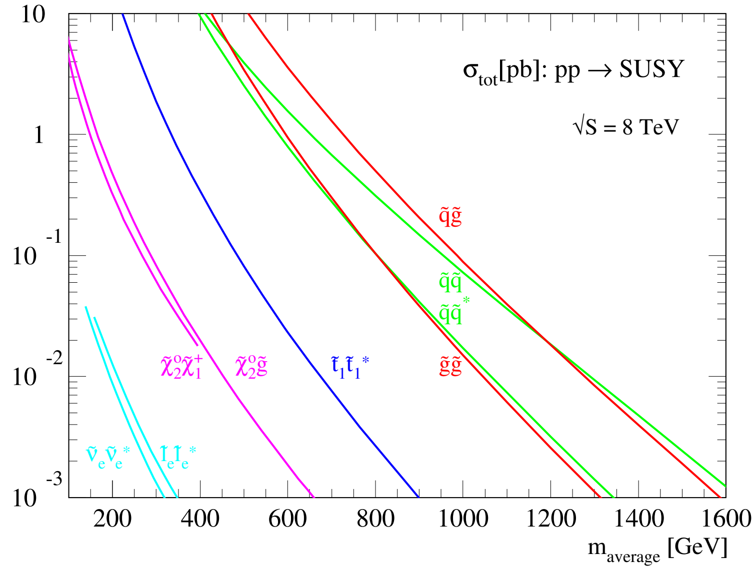

Fig. 13 Cross sections for SUSY particle production at $\sqrt{s} = 8$ TeV, based on Prospino. Particles with colour (squarks and gluinos) can be produced strongly and (for a given mass) have much larger cross sections than particles that can only be produced through electroweak interactions. However, the decay signatures of particles produced via electroweak processes can be quite distinctive, allowing sensitive searches to be performed. In this figure, an asterisk denotes an antiparticle, not an off-shell particle. Figure courtesy of Tilman Plehn.

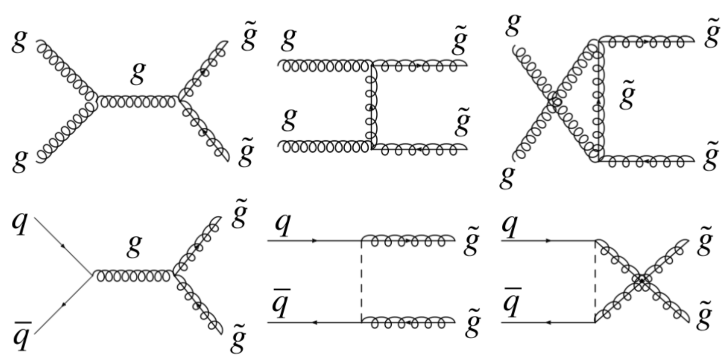

Fig. 14 Feynman diagrams leading to the production of a pair of gluinos in pp collisions in an R-parity-consverving SUSY model. The dashed lines in the intermediate state denote squarks.

$$\tilde{g} \to \tilde{b}_i^* \bar{b}, \qquad \tilde{b}_i^* \to b\tilde{\chi}_1^0, \tag{6}$$

where the $\tilde{b}^*$ indicates a virtual squark and i denotes either L,R or $1,2$. (Other possible squark decays are discussed below.) This decay sequence involves both a strong and a weak interaction vertex and leads to

$$\tilde{g} \to b\bar{b}\tilde{\chi}_1^0 \to \text{jet} + \text{jet} + E_T^{\text{miss}}. \tag{7}$$

Of course, if the two-body decay is allowed, the branching fraction for the three-body mode is highly suppressed.

Here is a simple question: How many gluino decay modes are there in LM6? For each of 5 flavours (u, d, c, s, and b) there are four modes (see Eq. 5). However, for top, there are only the two modes $\tilde{g} \to \tilde{t}_1\bar{t}$ and $\tilde{g} \to \bar{\tilde{t}}_1 t$, because $\tilde{t}_2$ is too heavy to be produced together with a t-quark. Thus, there are a total of 22 gluino decay modes in this model.

In SUSY models motivated by naturalness considerations, the $\tilde{t}_{L,R}$ and $\tilde{b}_L$ are typically constrained to be light, while the gluino is *not too heavy*. In pp collisions, stops can be produced in two main ways: (i) directly, via pair-production processes such as $gg \to \tilde{t}\bar{\tilde{t}}$, and (ii) indirectly, via gluino pair production $gg \to \tilde{g}\tilde{g}$, with $\tilde{g} \to \tilde{t}\bar{t} + \bar{\tilde{t}}t$. Because the production cross section for $\tilde{t}\bar{\tilde{t}}$ (or $\tilde{b}\bar{\tilde{b}}$) is much smaller than that for $\tilde{g}\tilde{g}$ (at the same mass), gluino pair production is a potentially useful way to search for stop and sbottom. Note also that, even if the $\tilde{b}_1$ mass turns out to be larger than that of $\tilde{t}_1$, the combined mass of the particles in the $\bar{t}\tilde{t}\bar{t}\tilde{t}$ final state could still be comparable to that in the $\tilde{b}\bar{b}\tilde{b}\bar{b}$ final state. There are many different possibilities to consider! We will discuss these scenarios in more detail in Section 6.2. Finally, we note that the $\tilde{u}$ and $\tilde{d}$ squarks, for which the corresponding quark flavour u and d is found in the proton, can be produced in additional processes. Inclusive hadronic searches (without b-tagging) place constraints on these squarks.

Several paradigms for squark decay are shown in Fig. 15. A squark can decay both via neutralino emission, as in $\tilde{b}_L \to b\tilde{\chi}_1^0$, and via chargino emission, as in $\tilde{b}_L \to t\tilde{\chi}_1^-$. Referring back to Fig. 12, let's consider the possible decays of $\tilde{t}_1$ and $\tilde{t}_2$ in LM6. The lighter mass eigenstate, $\tilde{t}_1$ has four possible decay modes: $\tilde{t}_1 \to t\tilde{\chi}_1^0$ (25%), $\tilde{t}_1 \to t\tilde{\chi}_2^0$ (16%), $\tilde{t}_1 \to b\tilde{\chi}_1^+$ (43%), and $\tilde{t}_1 \to b\tilde{\chi}_2^+$ (16%). The $\tilde{t}_2$ is significantly heavier and has four additional decay modes: $\tilde{t}_2 \to t\tilde{\chi}_3^0$, $\tilde{t}_2 \to t\tilde{\chi}_4^0$, $\tilde{t}_2 \to \tilde{t}_1 h$, and $\tilde{t}_2 \to \tilde{t}_1 Z$.

6.2 Examples of Searches for Supersymmetry

A typical SUSY search begins with a set of topological requirements for an appropriate set of reconstructed objects such as jets (or b-tagged jets), leptons, photons (especially in gauge-mediated SUSY), and E_T^{miss}. The term E_T^{miss} is confusing, because energy is not a vector and therefore cannot have a transverse component. This quantity is the magnitude of the missing transverse momentum vector,

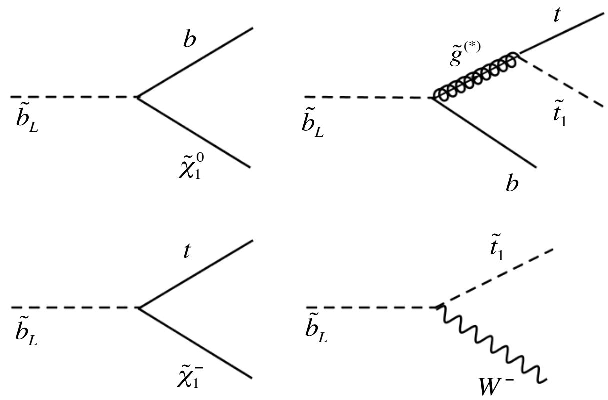

Fig. 15 Examples of diagrams for the decays of squarks (scalar quarks). The relative importance of the different processes depends on the particle masses, as well as on the the mixing parameters that determine the gaugino/higgino content of the charginos and neutralinos.

$E_T^{\text{miss}} = |\mathbf{p}_{\text{T}}^{\text{miss}}|$, where the *missing transverse momentum* is given by

$$\mathbf{p}_{\text{T}}^{\text{miss}} = -\left[\sum_{i=\text{objects}} \mathbf{p}_{\text{T}}^{i}\right]. \tag{8}$$

This calculation of $\mathbf{p}_{\text{T}}^{\text{miss}} = \mathbf{p}_{\text{T}}^{\text{init}} - \mathbf{p}_{\text{T}}^{\text{observed}}$ uses conservation of momentum and the fact that the initial-state momentum transverse to the beam direction is known to be zero to a very good approximation. (The energy label originates from the use of calorimeter measurements, which are important because the contributions of neutral particles, both photons and neutral hadrons, must be included.) An analogous calculation cannot be performed in the direction along the beams (z direction) because the colliding partons each carry unknown fractions (x_1 and x_2) of the proton momenta. If sufficiently well measured, E_T^{miss} and $\mathbf{p}_{\text{T}}^{\text{miss}}$ can be attributed to unobserved final-state particles.

The details of how the sum in Eq. 8 is performed over reconstructed objects are important. The objects can be jets above some minimum p_T threshold; in this case the variable is usually called MHT rather than E_T^{miss}. In an E_T^{miss} calculation, the objects are often calorimeter cells (both electromagnetic and hadronic) or calorimeter towers, combining different parts of the calorimeter that point back to the interaction point. In CMS, a particle flow technique is used in which information from the tracker and calorimeter is carefully combined to improve the resolution.

Figure 16 shows the E_T^{miss} resolution in ATLAS [71] as a function of another key global event variable, $\sum E_T$ (event), which is the *scalar sum* over the transverse momenta of the jets above threshold. ATLAS has used a variety of different control samples to measure the resolution, yielding consistent results that roughly follow a $\sqrt{\sum E_T}$ dependence (see figure). For backgrounds with large E_T^{miss} from neutrinos

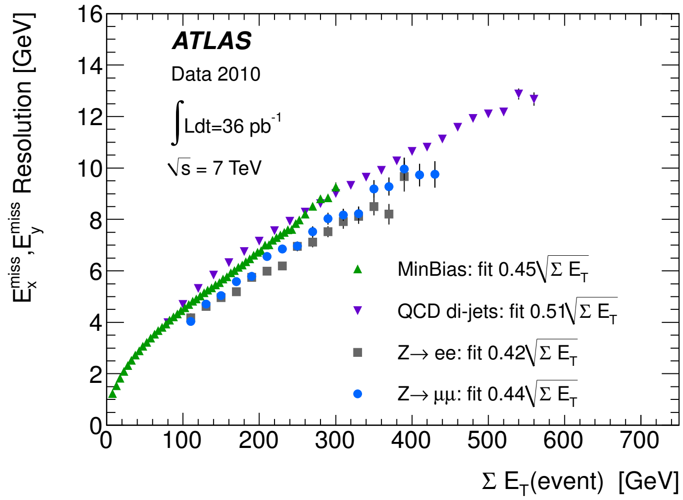

Fig. 16 Measured resolution on $E_T^{\rm miss}$ in the ATLAS experiment, using several different control samples. The results are consistent with $\sqrt{\sum E_T}$ dependence. From Ref. [71].

(such as leptonic $t\bar{t}$ events), the precise shape of the $E_T^{\rm miss}$ resolution function is usually not critical, because most of the $E_T^{\rm miss}$ in the event is genuine. But if there is substantial background from sources with fake $E_T^{\rm miss}$ (such as QCD multijet events), the effects of non-gaussian tails of the $E_T^{\rm miss}$ resolution function must be more carefully quantified. In CMS, a variety of specific instrumental effects that generate fake $E_T^{\rm miss}$ have been identified, and software filters have been developed to suppress such events.

The scalar sum of the jet transverse momenta (above some threshold, typically in the range 30–50 GeV) is usually denoted H_T (rather than $\sum E_T$),

$$H_T = \sum_{i=\text{jets}} p_T^i, \tag{9}$$

and is another discriminating variable commonly used in SUSY searches. Other interesting variables used in SUSY searches are α_T (discussed below), M_{T2} [72, 73], and the razor variables [74].

From the discussion in Section 6.1, it is clear that many SUSY production and decay scenarios can arise, and that a finely tuned optimization for each one is unwieldy. Partly for this reason, the initial SUSY searches performed by ATLAS and CMS were *inclusive*, based on simple topological signatures. These searches can be regarded as surveys to determine whether the event yields in the main channels are consistent with SM expectations. The main inclusive search topologies are

- Jets + $E_T^{\rm miss}$ (all-hadronic search; veto events with observed leptons)
- 1 lepton (e or μ) + jets + $E_T^{\rm miss}$

- 2 leptons + jets + E_T^{miss} (same-sign or opposite-sign leptons)
- 1 photon + jets + E_T^{miss}
- 2 photons + jets + E_T^{miss}
- ≥ 3 leptons + jets + E_T^{miss}

The like-sign dilepton channel and the trilepton channel are special in that SM backgrounds are highly suppressed. Although the number of expected signal events is typically very small for relevant SUSY models, the sensitivity can still be quite high. In the opposite-sign dilepton channel one can include a Z-boson selection. In all cases above, b-tagging can be used to define a search in a subsample of events with increased sensitivity to $\tilde{t}$ or $\tilde{b}$ decays.

6.2.1 SUSY and dark-matter searches in monojet final states

The first search that we will consider, however, has the amusing signature of $pp \rightarrow$ nothing, more or less. This is the simplest possible search–just look for nothing! This final state could correspond, for example, to the production of a pair of neutralinos, $pp \rightarrow \tilde{\chi}_i^0 \tilde{\chi}_j^0$. This is a weak process, so the cross section is small. For the case $i = j = 1$, this process is related to $\tilde{\chi}_1^0 p \rightarrow \tilde{\chi}_1^0 p$, which effectively corresponds to a (cosmic) direct dark-matter search. But while there is a strong motivation, it is obvious that one cannot perform this search quite as described. There is, however, a beautiful method, based on the fact that one can trigger on events with initial-state radiation, either a gluon or a photon. Both ATLAS [75, 76] and CMS [77, 78] have performed such searches. The collision after the radiation occurs can then proceed as before, but at a somewhat lower center-of-mass energy. Such processes lead to *monojet events*, which in fact are straightforward to find in the data. Figure 17 shows a monojet event from CMS. A highly energetic jet is recoiling against nothing, so there is a large amount of E_T^{miss}.

Does this mean that we have discovered SUSY? As always, the question is, what are the backgrounds? Unfortunately, the process $pp \rightarrow Z + 1$ jet, $Z \rightarrow \nu\bar{\nu}$ produces monojet events, and there is a smaller background from $W + 1$ jet as well. (It is possible to suppress $t\bar{t}$ and QCD multijets backgrounds to a very low level.) The Z background is measured in data by scaling the yields from a $Z \rightarrow \mu^+\mu^-$ control sample. Figure 18 shows the distribution of E_T^{miss} from an ATLAS monojet search. Searches by both ATLAS and CMS have produced remarkably sensitive results. With some care, such LHC results can be translated into the type of dark matter exclusion plots (cross section vs. WIMP mass) obtained from direct dark-matter detection experiments [79, 80].

Even if an excess with respect to the SM were observed, one should not jump to the conclusion that SUSY is the explanation. Many signatures for new physics can admit more than one explanation. The "problem" of identifying which kind of new physics is the actual source of an observed excess is the kind of problem we want to have!

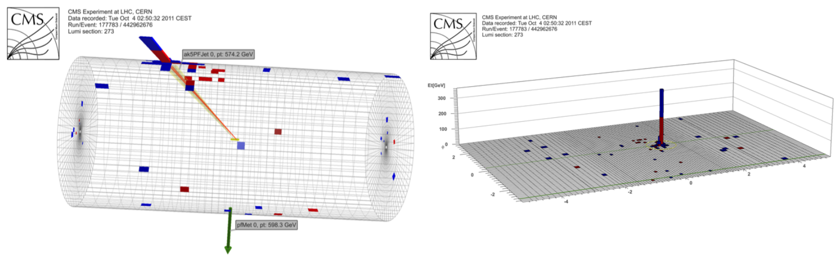

Fig. 17 Event display for a monojet event in the CMS experiment, showing the energy desposited in the electromagnetic calorimeter (red) and the hadronic calorimeter (blue). There are many monojet events in the data sample, but this does not mean that SUSY has been discovered!

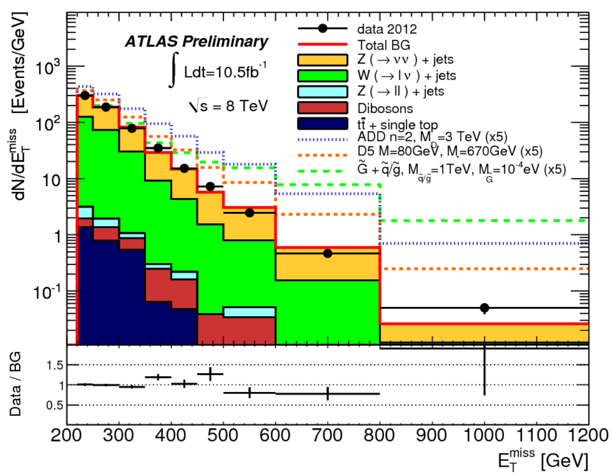

Fig. 18 ATLAS monojet search: observed distribution of E_T^{miss} in data (points with error bars), together with expected SM backgrounds (stacked histograms) and expectations from various signal hypotheses. Note that the dominant background arises from $Z+$ jets, with $Z \to \bar{\nu}\nu$. The x-axis of the plot begins at 200 GeV. From Ref. [75].

6.2.2 SUSY searches in all-hadronic final states

Searches in the dijet + E_T^{miss} or multijets + E_T^{miss} channel are sensitive to production of SUSY particles via strong interactions. For example, the production of a pair of squarks can lead to a dijet + E_T^{miss} final state via the process $pp \to \tilde{q}\bar{\tilde{q}}$ with $\tilde{q} \to q\tilde{\chi}_0^1$. This final state has an enormous background from QCD dijet events. The jets in such background events, however, are typically back to back with equal energies. A variable that measures these characteristics is [81],

$$\alpha_T = \frac{p_T^{j_2}}{M_T(j_1, j_2)} = \frac{\sqrt{p_T^{j_2}/p_T^{j_1}}}{\sqrt{2(1-\cos\Delta\phi)}}, \tag{10}$$

which has been used to dramatically suppress the QCD dijet background [82]. (It has also been generalized to treat multijet events by forming two pseudo-jets.) Here, j_1 and j_2 are the first- and second-leading jets in p_T and $\Delta\phi$ is the angle between them in the transverse plane. Well-measured QCD dijets events are balanced ($\alpha_T = 0.5$), while SUSY events such as $\tilde{q}\bar{\tilde{q}}$ production often have $\alpha_T > 0.5$. *Mismeasured* QCD events usually have $\alpha_T < 0.5$.

Several strategies have been used to study the multijets + E_T^{miss} channel. Although Z + jets and $t\bar{t}$ are the dominant backgrounds at high E_T^{miss}, it is critical to have a reliable measurement of the QCD multijet background as well. Figure 19 shows the H_T and missing H_T distributions from a CMS search [83] in this channel, after the application of a basic set of preselection requirements. (Missing H_T is calculated using jets rather than calorimeter cells and is better suited to the data-driven QCD background estimation method used in this analysis, which involves a jet-energy-smearing procedure.) The preselection requires at least three jets with $p_T > 50$ GeV and $|\eta| < 2.5$, and events are vetoed if they contain an isolated lepton with $p_T > 10$ GeV. Because fake E_T^{miss} in QCD multijet events is usually associated with a single, badly mismeasured jet, the E_T^{miss} in such events is usually aligned with a jet; this background can therefore be suppressed with the requirement $\Delta\phi(\mathbf{p}_T^{\mathrm{miss}}, j_1) > 0.5$, where j_1 is the leading jet. (Similar cuts are applied to the second and third leading jets.)

Both of the kinematic variables H_T and missing H_T provide sensitivity to a SUSY contribution, which is shown overlaid on the stacked histograms for the background predictions. In the missing H_T distribution, the QCD multijet contribution falls off more rapidly than the other backgrounds, which produce genuine E_T^{miss} associated with neutrinos. The contribution from $Z \to \nu\bar{\nu}$+jets is critical (see Fig. 19) and is measured with a γ+jets control sample. While $Z \to \mu^+\mu^-$+jets provides an alternative method, the small branching fraction for leptonic Z decay is a severe limitation in the statistical power of the control sample. Theoretical support for this method has been important to relate the γ+jets control sample to the Z+jets background. In this search, essentially all backgrounds are determined with data-driven methods, and the observed yields in the signal regions are consistent with the background predictions.

6.2.3 SUSY searches in final states with leptons

SUSY processes generate many different signatures with leptons. In the SM, leptons can be produced in processes mediated by γ, Z, $W^{\pm}$, and Higgs bosons, but not by gluons. Because SUSY preserves gauge quantum numbers, an analogous statement holds in SUSY models. Sleptons (scalar leptons) and sneutrinos can be produced directly in electroweak processes (with small cross sections, as shown in Fig. 13), or in the cascade decays of other SUSY particles, once either electoweak gauge

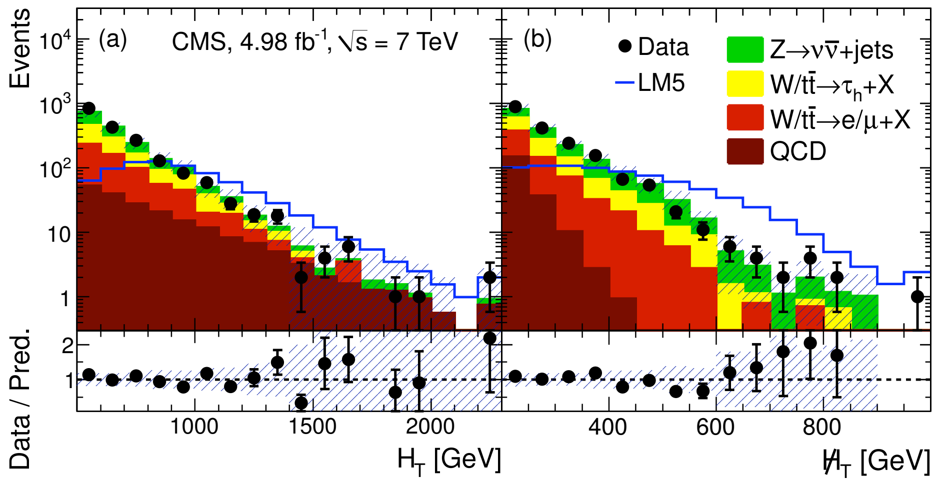

Fig. 19 CMS experiment: distributions of H_T, the scalar sum of jet p_T values, and missing H_T in a search for SUSY in the multijets + E_T^{miss} channel. The SM backgrounds are displayed as stacked histograms, while the expectation for the SUSY LM5 benchmark model is shown as an overlaid histogram. Because the logarithmic scale can sometimes hide discrepancies, it is useful to compare the data with the predicted SM background on a linear scale, as shown below the main histograms. From Ref. [83].

bosons or their SUSY partners are produced (either on- or off-shell). Figure 12 shows that squark decays can lead to the production of neutralinos or charginos. The neutralinos can decay via processes such as $\tilde{\chi}_2^0 \to \tilde{\ell}_{L,R}^{\pm}\ell^{\mp}$, $\tilde{\chi}_2^0 \to \tilde{\nu}\bar{\nu}$, $\tilde{\chi}_2^0 \to \bar{\tilde{\nu}}\nu$, $\tilde{\chi}_2^0 \to \tilde{\chi}_1^0 h$, and $\tilde{\chi}_2^0 \to \tilde{\chi}_1^0 Z$. The charginos can decay via processes such as $\tilde{\chi}_1^+ \to \tilde{\nu}_{\ell L}\ell^+$, $\tilde{\chi}_1^+ \to \tilde{\ell}_L^+\nu$, and $\tilde{\chi}_1^+ \to \tilde{\chi}_1^0 W^+$. When neutralinos and charginos (or W and Z bosons) are produced, leptonic signatures become important.

Decays of $\tilde{\chi}_i^0$ and $\tilde{\chi}_j^{\pm}$ give rise to some of the most famous SUSY signatures. The decay of the heavy neutralino can proceed through the cascade,

$$\tilde{\chi}_2^0 \to \tilde{\ell}^{\pm}\ell^{\mp},\ \tilde{\ell}^{\pm} \to \ell^{\pm}\tilde{\chi}_1^0, \tag{11}$$

where the first decay is analogous to $Z \to \ell^+\ell^-$. The scalar lepton $\tilde{\ell}$ can be either on- or off-shell; its decay preserves the flavour of the original lepton-slepton pair, so the two final-state leptons have opposite sign and same flavour. The distribution of invariant masses of the dilepton system is a powerful tool that is unusual in SUSY searches. Although there is no peak in this mass spectrum, it has important kinematic features, including a well-defined upper edge.

One of the most basic leptonic SUSY searches involves a signature with a single lepton, jets, and E_T^{miss}. As it happens, one of the students at this school, Jeanette Lorenz, has been closely involved in such a search on ATLAS. We consider her paper [84] as an example. The analysis requires at least four jets with $p_T > 80$ GeV and one isolated lepton with $p_T > 25$ GeV. Events are vetoed if there is a second isolated lepton with $p_T > 10$ GeV. This requirement helps to suppress $t\bar{t}$ dilepton events. Of course, SM events with a single lepton, jets, and E_T^{miss} arise from $t\bar{t}$ events or from W+jets events, with a leptonic $W \to \ell\bar{\nu}$ decay in either case. Such true single-lepton events in which both the lepton and neutrino are produced in the decay of a single W boson can be suppressed using the transverse mass quantity,

$$m_T \equiv \sqrt{2p_T^{\ell}E_T^{\mathrm{miss}}(1-\cos\Delta\phi)}, \tag{12}$$

where the lepton mass has been ignored and ϕ is the angle between the lepton and the E_T^{miss} vector in the transverse plane. When the lepton and the E_T^{miss} in an event both arise from $W^- \to \ell^-\bar{\nu}$ decay, m_T approximates the mass of the lepton-neutrino system, and the distribution of m_T cuts off around the W boson mass. In contrast, the m_T distribution in many SUSY models extends well above the W mass because the source of E_T^{miss} is χ_1^0 production, which is effectively decoupled from the lepton.

A key ingredient of Jeanette's analysis is the use of several control regions, which are used to monitor the main backgrounds. These regions are cleverly defined using b-tagging and anti-b-tagging to separate the $t\bar{t}$ and W+jets contributions. The regions are defined in a region of intermediate E_T^{miss} to suppress potential contamination from a SUSY signal. As a perspective on the degree of background rejection involved in such an analysis, I estimate from Jeanette's paper that, comparing the number of $W \to \ell\bar{\nu}$+jets events produced to the number contributing to the signal region, the rejection factor is around 3×10^{-7}, while for single-lepton $t\bar{t}$, the rejection factor is around 2×10^{-4}. These impressive factors give an idea of how SUSY searches must strongly suppress SM backgrounds. CMS results for the single-lepton final state are presented in Ref. [46].

6.2.4 Interpreting SUSY results

Many ATLAS and CMS searches, especially the initial studies, were interpreted using the constrained Minimal Supersymmetric Standard Model (cMSSM). This framework provides a means to compare results with searches from the Tevatron and LEP. The cMSSM contains just five parameters, which are defined at the grand unification (GUT) scale: a common scalar fermion mass (m_0), a common gaugino mass ($m_{1/2}$), a common trilinear coupling (A_0), the ratio of vacuum expectation values for u- and d-type fermions ($\tan\beta$), and the sign of the higgsino mass parameter (sign μ). Figure 20 shows the excluded region in the $m_{1/2}$ vs. m_0 plane for fixed values of the other cMSSM parameters, which are specified at the top of the figure.

These plots can be mysterious, but it is useful to note that the contour lines of fixed gluino mass are nearly horizontal, with $m(\tilde{g}) \approx 2.5m_{1/2}$, while the contours of fixed squark mass have more curvature, but are roughly vertical for large values of m_0. To produce an exclusion plot of this type, it is necessary to generate simulated event samples for the signal at a grid of model points covering the parameter space of the plot. For each point, one determines whether the signal yield predicted for the given SUSY model parameters (using the predicted cross section, usually at NLO)

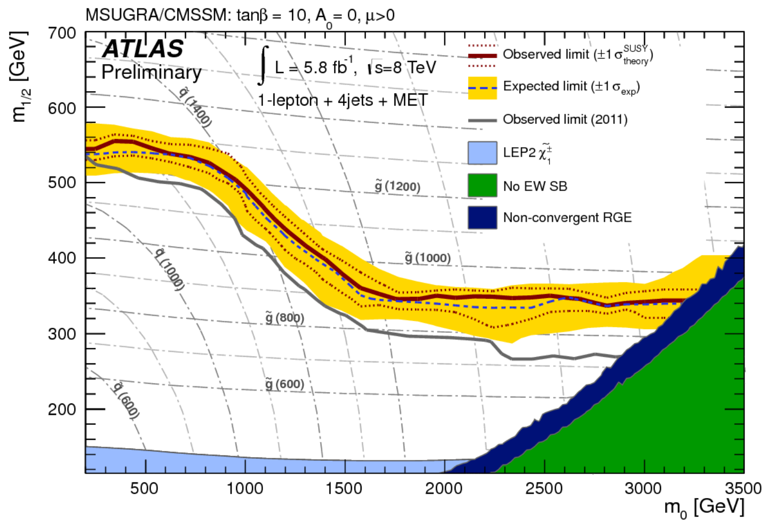

Fig. 20 Exclusion region in the $m_{1/2}$ vs. m_0 plane of the cMSSM from an ATLAS search for SUSY in the single lepton + jets + E_T^{miss} channel. From Ref. [84].

can be excluded on the basis of the observed event yield in data, taking into account the predicted SM background. We can see that Jeanette's analysis excludes gluino masses below 0.9–1.3 TeV (roughly), depending on the value of m_0.

While the GUT-scale constraints increase the predictive power of the cMSSM (and allow us to make beautiful plots), many theorists regard these constraints with some suspicion. In addition, the contraints lead to relationships between SUSY particle masses at the electroweak scale that are not sufficiently generic to cover the ranges of all important scenarios. A gluino mass excluded in the context of a cMSSM interpretation might not be excluded in a more generic model that permits a broader range of mass splittings. Small mass splittings generally lead to less E_T^{miss} and/or softer jets, and therefore to lower signal efficiencies and poorer sensitivity.

As noted earlier, the framework of *simplified models* has been developed to provide a more generic description of relevant new physics processes. Figure 21 show several examples of (the many) models that can be defined defined within this framework. Each model describes a single production and a single decay chain; a null result from a search can be used to place an upper limit on the cross section that can be associated with the full process. For a given set of mass parameters, one can also calculate a reference cross section for the simplified model that can be tested against observations in data. This allows one to exclude the given set of parameters. Note, however, that if the same mass values are embedded in a complete SUSY spectrum, the branching fractions can very well change because additional decay channels can become available. This effect can weaken the mass constraints. Simplified models

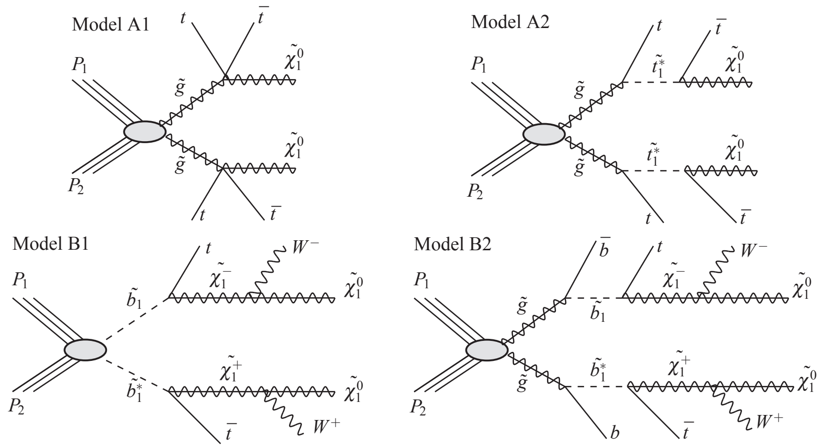

Fig. 21 Simplified models used for the CMS like-sign dileptons + b jets search. Model A1 corresponds to gluino pair production with decays to off-shell stop; model A2 is similar with gluino decay to on-shell stop. Model B1 corresponds to direct production of sbottom, and model B2 corresponds to gluino pair production followed by production of sbottom. From Ref. [86], a CMS search for like-sign dileptons with b jets. In this figure an asterisk (*) denotes an antiparticle, not an off-shell particle.

have been especially useful for studies motivated by naturalness, where the number of relevant SUSY particles is typically small.

6.2.5 SUSY searches motivated by naturalness

The concepts of *fine tuning* and *naturalness* were described in the introduction, and they have been discussed extensively in the literature. The discovery of a Higgs-like particle at $m \sim 125$ GeV has strengthened what were previously hypothetical arguments, and it is now more urgent to confront the question of whether and how the mass of this spin-0 particle is protected against enormous quantum corrections. A neutral way to formulate this question is to say that we would like to determine experimentally whether nature is fine tuned and, if not, to identify the mechanism that avoids the need for fine tuning. Models for new physics beyond the SM that avoid fine tuning are called *natural models,* and they include SUSY models with certain characteristics that we discuss here.

The paper *Natural SUSY Endures* [13] provides a useful starting point to learn about these issues. (A student at this school, C.-T. Yu, is also a co-author of a recent paper on related natural SUSY phenomenology [85].) The implications of naturalness can be found by analyzing the effects that contribute to the quadratic terms in the Higgs potential, including higher order corrections from gauge and Yukawa interactions. Naturalness can be interpreted to mean that such terms are similar in size, with magnitudes set by the electroweak scale ($v \sim 246$ GeV). In the context of SUSY, these considerations lead to the following conclusions:

1. the masses of $\tilde{t}$ (both stops) and $\tilde{b}_L$ (but not $\tilde{b}_R$) are less than 500–700 GeV,
2. the gluino is not too heavy, below 900 GeV – 1.5 TeV, and
3. the higgsinos ($\tilde{H}$) are also light, leading to one chargino and two neutralinos with masses less than 200 – 350 GeV. Neutralino and chargino states are designated collectively as electroweakinos or EWKinos.

The masses of the other SUSY partners do not play an important role in suppressing the Higgs quantum corrections and so are much less constrained. Their masses could be greater than 10 TeV and not affect fine-tuning considerations. As a consequence, many recent SUSY searches have focused on the states listed above. Both direct production of squark-antisquark pairs and indirect production via gluino decays are important channels; gluino pair production has a larger cross section if the gluino mass is not too large.

The production and decays of SUSY particles was discussed in Sec. 6.1. A key point is that the cross section for direct pair production of squarks is very small, unless their SM partners are valence quarks in the proton (see Fig. 13). Searches for $\tilde{t}\bar{\tilde{t}}$ and $\tilde{b}\bar{\tilde{b}}$ must therefore contend with small cross sections. Note that, because squarks are scalars, their direct production cross sections are suppressed relative to those for fermion pair production because there is only one spin state to sum over. The contribution to squark pair production from $q\bar{q} \to \tilde{t}\bar{\tilde{t}}$ is also suppressed near threshold by the factor β^3 (where β is the velocity of the $\tilde{t}$), because the $\tilde{t}\bar{\tilde{t}}$ must be produced in an $\ell = 1$ state (p-wave). Finally, squark production is suppressed relative to gluino production because of the different colour factors for the two cases. Besides the small cross sections, an additional challenge arises in direct-production searches: kinematically, the $t\bar{t}$ background shares many of the overall features of the $\tilde{t}\bar{\tilde{t}}$ signal.

In spite of these challenges, significant progress has been made using the $\sqrt{s} = 8$ TeV data sample to search for light stop, sbottom, and EWKinos. Figure 22 shows the results from ATLAS searches for direct stop production (incorporating updates after this school). The excluded scenarios are regions in the $m(\tilde{\chi}_1^0)$ vs. $m(\tilde{t}_1)$ plane, and are based on searches in zero lepton, one lepton, and dilepton final states. The use of b-tagging plays a major role in these searches; fortunately this tool is very well developed in both ATLAS and CMS. Figure 22 is divided into two parts, according to the stop decay channel assumed. The process $\tilde{t}_1 \to b\tilde{\chi}_1^{\pm}$, $\tilde{\chi}_1^{\pm} \to W^{(*)}\tilde{\chi}_1^0$ is assumed for the exclusion regions shown on the left, while the decay $\tilde{t}_1 \to t\chi_1^0$ is shown on the right. Sensitivity to $\tilde{t}\bar{\tilde{t}}$ production cuts off at large $\tilde{t}_1$ masses because of the corresponding fall off in cross section. Sensitivity also falls off as the $\tilde{\chi}_1^0$ mass increases, because the spectrum becomes *compressed*, resulting in small values of E_T^{miss} and softer jets. For model parameters near the diagonal in this plot, the results are sensitive to initial-state radiation, which affects the high end of the E_T^{miss} distribution. The presentation of the search results for light stop is reasonably well suited to the simplified models approach. However, the results shown in Fig. 22 incorpo-

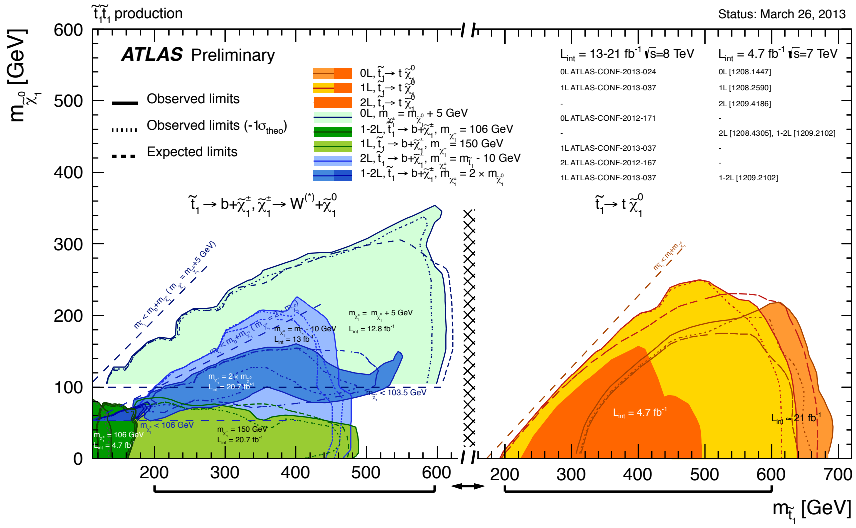

Fig. 22 ATLAS limits on direct stop production. The left-hand part of the figure shows limits obtained from searches for $\tilde{t}_1 \rightarrow b\tilde{\chi}_1^{\pm}$, $\tilde{\chi}_1^{\pm} \rightarrow W^{(*)}\tilde{\chi}_1^0$, while the right-hand part shows limits obtained from searches for $\tilde{t}_1 \rightarrow t\tilde{\chi}_1^0$.

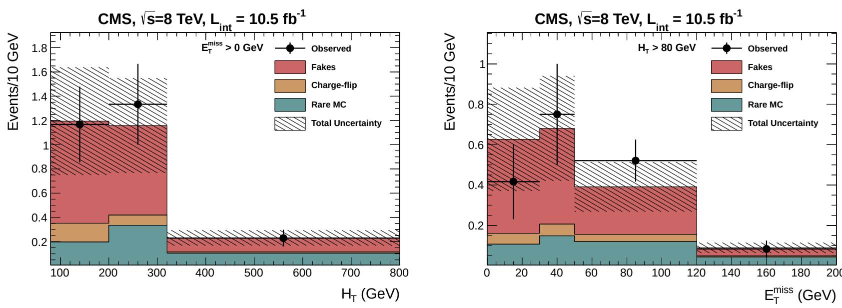

Fig. 23 CMS experiment: distributions of H_T and E_T^{miss} for events with like-sign dileptons and b-jets. From Ref. [86].

rate several assumptions and the interested reader should refer to the original papers for more information.

Figure 23 shows results from a search for light-stop search from CMS [86] in the final state with like-sign dileptons + b-jets. Pairs of isolated like-sign leptons are rare in SM processes. They can arise from processes in which one lepton is primary, from W-boson decay, and the second is secondary, for example, from b decay. Most of the secondary leptons are not isolated (they are inside or near b-jets), but some are. In addition, effects such electron charge misidentification as a result of bremsstrahlung must also be understood. Finally, there are a small number of rare SM processes that actually produce same-sign dileptons, such as $t\bar{t}Z$ and $t\bar{t}W$. The CMS search considers events with two isolated leptons (e or μ) with $p_T > 20$ GeV, at least two b-tagged jets with $p_T > 40$ GeV, and large $E_T^{\rm miss}$. Figure 23 shows the distributions of H_T and $E_T^{\rm miss}$ for the events satisfying these criteria: the data are consistent with the background predictions. (The ATLAS results are presented in Ref. [87].) As we noted before in the context of monojet searches, a signal in a final-state such as like-sign dileptons would not point to a unique source of new physics. In fact, the absence of any signal so far has been used to establish limits on several SUSY scenarios, including sbottom pair production, gluino pair production with off-shell stops, and gluino pair production with on-shell stops.

Let's briefly consider pair production of neutralinos and charginos (EWKinos). Because these particles do not have colour charge, the cross sections are generically much smaller than those for gluinos and squarks. On the other hand, the signatures can be distinctive, and it is possible that the EWKino masses are small, boosting their cross sections. We have already discussed the famous neutralino cascade process $\tilde{\chi}_2^0 \to \tilde{\ell}^{\pm}\ell^{\mp}$, $\tilde{\ell}^{\pm} \to \ell^{\pm}\tilde{\chi}_1^0$ that gives rise to a pair of opposite-sign, same flavour leptons. An even more distinctive signature is that of trileptons, which can be produced in processes such as $pp \to \tilde{\chi}_1^{\pm}\tilde{\chi}_2^0$. SM processes rarely produce three isolated primary leptons; the analysis must therefore carefully measure the contribution from events with at least one "fake lepton" (which can in fact be a lepton from semileptonic b-quark decay).

7 Exotica Searches

This section describes examples of searches that have novel features, either in their methodologies or in their physics goals. These examples highlight the fact that the range of possibilities at the TeV scale is vast, and we must try to investigate as many of them as possible.

7.1 Search for Large Extra Dimensions

As noted in the introduction, SUSY is not the only approach to resolving the hierarchy problem: both extra spatial dimensions and technicolour provide alternatives. In fact, the monojet search discussed in connection with a search for neutralino pair production can also be interpreted in the context of models of extra dimensions. How is that? Let's start with the model of Arkani-Hamed, Dimopoulos, and Dvali (ADD) [25], which provides a completely different approach to the hierarchy problem from that of SUSY. This model postulates that in a fundamental sense, there is no difference between the weak scale and that of gravity, once gravity is properly understood. The idea is that gravity appears to us to be extremely weak (and the associated Planck scale $M_{\rm Pl}$ appears to be correspondingly very high, creating the huge difference with respect to the electroweak scale) because gravity (and not the other forces) propagates in additional dimensions besides those that we observe. In Large Extra Dimensions (LED) models, n extra spatial dimensions of size R are postulated; the "true" Planck scale in $4+n$ dimensions is given by $M_D^{2+n} = M_{\rm Pl}^2/R^n$, which can be made compatible with the electroweak scale by making R sufficiently large. (The hierarchy problem is then translated into a new question about why R or n is so large.)

The LED hypothesis has motivated challenging measurements of gravity at submillimeter distance scales. Furthermore, because the true, higher dimensional gravity is strong at the electroweak scale, it should be possible to produce gravitons in LHC collisions. The compactification of the extra dimensions results in a Kaluza-Klein "tower" of massive graviton excitations. Because the gravitons propagate in the extra dimensions, they can escape detection, leading to an $E_T^{\rm miss}$ signature similar to that from SUSY models. Studies of monojet and monophoton events have yielded limits that exclude values of M_D below ~ 3 TeV for n in the range 2–6 [75, 76, 77, 78].

A more modern but related idea, the Randall-Sundrum (warped extra dimension) model [24], requires just one extra dimension. In this model, the extra dimension separates two $3+1$ dimensional surfaces (branes) in the full higher-dimensional space. Gravity is concentrated on one brane, while the particles of the SM reside on the other. Gravity can propagate in the bulk region between the two branes, but it is exponentially attenuated. It is this attenuation that makes gravity appear weak, rather than the dilution effect that operates in LED models. As in the case of LED, a Kaluza-Klein tower of graviton modes is produced, but in this case the decay signature does not involve large $E_T^{\rm miss}$. Gravitons can be produced in $q\bar{q}$ or gg s-channel processes and then decay into pairs of SM particles, including photons [88].

7.2 Search for Long-lived Stopping Particles

Imagine a particle that lives long enough that it does not decay during the beam crossing interval when it was produced, but simply stops somewhere in the detector and eventually decays. Such particles are predicted in a variety of different scenarios, including hidden valley models [89, 90] and models with split supersymmetry [91, 92]. Let's consider a split SUSY scenario, in which the gluino and neutralino (LSP) have masses at the LHC energy scale but all of the scalar SUSY particles are at some extremely high mass scale. The gluino then has a long lifetime, because the two-body decay $\tilde{g} \to \tilde{q}\bar{q}$ is forbidden. Possible decays are $\tilde{g} \to g\tilde{\chi}_1^0$, which must proceed via a loop diagram since the neutralino has no colour, and $\tilde{g} \to q\bar{q}\tilde{\chi}_1^0$. A process to compare in the SM is the β decay of a free neutron, $n \to pe^-\bar{\nu}_e$, which leads to the neutron lifetime of about 10 minutes.

What happens to a long-lived gluino? As a consequence of its long lifetime, it hadronizes into an object called an R-hadron, which can be $\tilde{g}g$, $\tilde{g}q\bar{q}$, $\tilde{g}qqq$, and so on. The R-hadron interacts with the material in the detector and, some fraction of

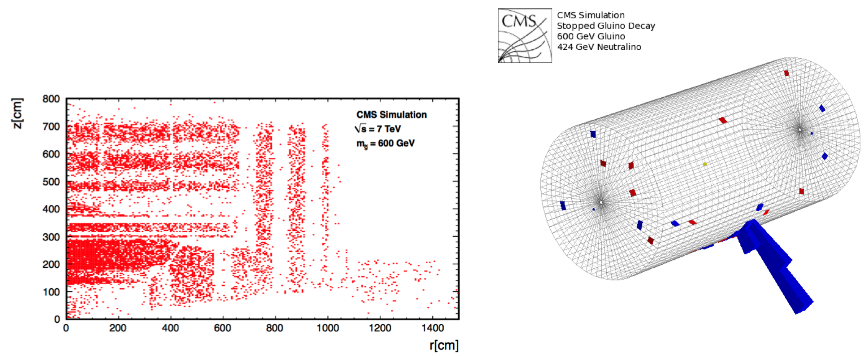

Fig. 24 CMS experiment: search for *R*-hadrons. Left: a map of the densest regions of the detector, where *R*-hadrons are most likely to stop. Right: a simulated *R*-hadron decay. Note that the pointing direction of the displayed calorimeter tower is not meaningful in the context of this search.

the time, will stop, typically in the densest region. Figure 24 (left) shows a map of these regions in CMS.

The first question to ask ourselves is whether we would even trigger on such events. Remember the fundamental principle: "If it didn't trigger, it didn't happen." In other words, without a suitable trigger, the event will be lost forever and you might as well not have built the detector. Not good! In CMS a special trigger was implemented to search for energy deposits ($p_T > 50$ GeV) in the calorimeter that were present in the intervals between beam crossings (vetoing on signals from the beam position monitors on either side of the CMS detector) [93]. In a fill with 228 bunches per beam, 85% of each orbit period (89 μs) was available for the search, falling to 16% of the orbit period for a fill with 1380 bunches.

Remarkably, it was possible to suppress backgrounds from sources such as beam-halo events, cosmic rays, and calorimeter noise to a very low level, around 1.5×10^{-6} Hz. Limits on various stopping particles are then obtained as a function of the particle masses and lifetimes [93].

7.3 Search for Microscopic Black Holes

The intriguing possibility of producing microscopic black holes at the LHC has attracted much attention, both in and outside the physics community. The production of black holes would be a signature of low-scale quantum gravity. There are many possible scenarios, leading to a small industry of models and accompanying simulation programs. The phenomenology of black-hole formation involves several subtleties, such as defining the fraction of the initial parton energy that is trapped within the event horizon, whether the black hole is rotating or not, whether there is a stable remnant, and so on. Black hole searches are based on signatures with rather

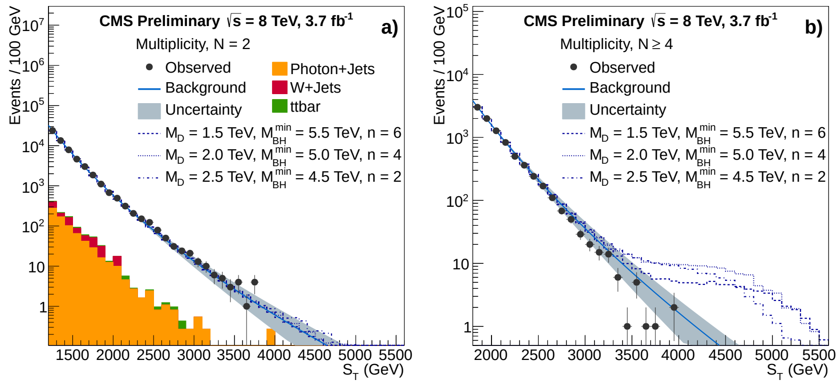

Fig. 25 Kinematic distributions from a CMS search for black holes. The S_T variable is the scalar sum of the p_T values over essentially all objects (jets, isolated leptons, isolated photons, E_T^{miss}) in the event. The multiplicity N includes all objects except E_T^{miss}. Left: low-multiplicity ($N = 2$) control region. Right: example of a high-multiplicity ($N \geq 4$) signal region, with simulated black-hole signals.

broad interest, which involve events with very large total transverse energy and high particle multiplicity.

CMS has performed a black hole search [94] based on the kinematic variable S_T, which is the scalar sum of the transverse momenta of essentially all objects including E_T^{miss},

$$S_T = \sum_{i=j,\ \ell,\ \gamma,\ E_T^{\text{miss}}} p_T^i, \tag{13}$$

where j represents jets, ℓ represents isolated leptons, and γ represents isolated photons. Thresholds are applied to all objects. Distributions of S_T in 8 TeV data are shown in Fig. 25; these distributions extend beyond 3 TeV. The background shape is obtained from a fit to low-multiplicity (N, where N does not include E_T^{miss})) events in data, with the restriction $1200 < S_T < 2800$ GeV. The shapes in the $N = 2$ and $N = 3$ samples are very similar, and a dedicated search for new physics in the $N = 2$ sample shows no signal. Figure 25 shows an example of a high-multiplicity sample, $N \geq 4$. The data are well described by the background shape, and black-hole signal shapes are included for reference. This study excludes black hole masses below 4–6 TeV, depending on the model.

8 Conclusions

With the LHC, we have an extraordinary tool for exploring the deep issues of electroweak unification and the Higgs sector, the mystery of the gauge hierarchy problem, and the nature of dark matter. In addressing these and other questions, we may (or may not) discover supersymmetry, extra dimensions, and new forces of nature. At a more basic level, the operations of the LHC at 7 TeV and 8 TeV have been remarkably smooth. The upcoming run at 13 TeV promises to be one of the most important periods in the history of particle physics. There are no guarantees, but the potential for breakthroughs has never been greater. Your work and leadership will be critical in achieving these goals.

Acknowledgements I would like to express my deep thanks to all of the organizers and staff at the *69th Scottish Universities Summer School in Physics*. Their superb hospitality and hard work made the school a great success. The graduate students and postdocs at the school were outstanding, and I would like to thank them for their enthusiasm, advice, interest, and willingness to perform my skit, *Higgs in Hollywood*, at the banquet. I would also like to thank Robert Cahn and Jonathan Feng for their helpful advice. Finally, I would like to thank several of my UCSB colleagues and students for their many comments on the manuscript: Mark Srednicki, David Stuart, Manuel Franco Sevilla, Tom Danielson, Kristen Flowers, Adam Dishaw, and Jack Bradmiller-Feld.

References

1. G. Aad *et al.* [ATLAS Collaboration], Phys. Lett. B **716** (2012) 1.
2. S. Chatrchyan *et al.* [CMS Collaboration], Phys. Lett. B **716** (2012) 30.
3. F. Englert and R. Brout, Phys. Rev. Lett. **13** (1964) 321.
4. P. W. Higgs, Phys. Lett. **12** (1964) 132.
5. P. W. Higgs, Phys. Rev. Lett. **13** (1964) 508.
6. G. S. Guralnik, C. R. Hagen and T. W. B. Kibble, Phys. Rev. Lett. **13** (1964) 585.
7. G. Aad *et al.* [ATLAS Collaboration], JINST **3** (2008) S08003.
8. S. Chatrchyan *et al.* [CMS Collaboration], JINST **3** (2008) S08004.
9. See for example T. D. Lee, *Particle Physics and Introduction to Field Theory*, (Harwood Academic Publishers, London, 1981), pp. 207-208.
10. C. Amsler, T. DeGrand, B. Krusche, Quark Model, in J. Beringer *et al.* [Particle Data Group Collaboration], Phys. Rev. D **86** (2012) 010001.
11. H. E. Haber, Supersymmetry, Part I (Theory), in J. Beringer *et al.* [Particle Data Group Collaboration], Phys. Rev. D **86** (2012) 010001.
12. P. Binétruy, *Supersymmetry: Theory, Experiment and Cosmology* (Oxford University Press, Oxford, 2006), p. 9.
13. M. Papucci, J. T. Ruderman and A. Weiler, JHEP **1209** (2012) 035.
14. G. F. Guidice, in Perspectives on LHC Physics, edited by G. Kane and A. Pierce (World Scientific, Singapore, 2008), p. 155.
15. J. L. Feng, Ann. Rev. Astron. Astrophys. **48** (2010) 495.
16. G. Bertone, D. Hooper and J. Silk, Phys. Rept. **405** (2005) 279.
17. D. Hooper, TASI2008 Lectures on Dark Matter, in *The Dawn of the LHC Era, Proceedings of the 2008 Theoretical Advanced Study Institute in Elementary Particle Physics*, Boulder, Colorado, 2–27 June 2008, ed. by Tao Han (World Scientific, Singapore, 2009).
18. Y. .A. Golfand and E. P. Likhtman, JETP Lett. **13** (1971) 323.

19. D. V. Volkov and V. P. Akulov, Phys. Lett. B **46** (1973) 109.
20. D. V. Volkov and V. A. Soroka, JETP Lett. **18** (1973) 312.
21. J. Wess and B. Zumino, Nucl. Phys. B **70** (1974) 39.
22. K.A. Olive, S. Rudaz, and M.A. Shifman, eds. Proceedings of the International Symposium Celebrating 30 Years of Supersymmetry. *Nucl. Phys.* B101 (Proc. Suppl.), 2001.
23. S. P. Martin, A Supersymmetry Primer, arXiv:hep-ph/9709356.
24. L. Randall and R. Sundrum, Phys. Rev. Lett. **83** (1999) 3370.
25. N. Arkani-Hamed, S. Dimopoulos and G. R. Dvali, Phys. Lett. B **429** (1998) 263.
26. I. Aitchison, *Supersymmetry in Particle Physics* (Cambridge University Press, Cambridge, 2007).
27. H. Baer and X. Tata, *Weak Scale Supersymmetry* (Cambridge University Press, Cambridge, 2006).
28. M. Drees, R. Godbole and P. Roy, *Theory and Phenomenology of Sparticles* (World Scientific, Singapore, 2004).
29. J. Wess and J. Bagger, *Supersymmetry and supergravity*, (Princeton University Press, 1992).
30. O. Buchmuller and P. de Jong, Supersymmetry, Part II (Experiment), in J. Beringer *et al.* [Particle Data Group Collaboration], Phys. Rev. D **86** (2012) 010001.
31. D. Green, *At the Leading Edge: The ATLAS and CMS LHC Experiments* (World Scientific, Singapore, 2010).
32. B. Niczyporuk, representing the Crystal Ball Collaboration, in: P. McDonough (ed.), *Proceedings of the 12th SLAC Summer Institute on Particle Physics*, Stanford, California, 1984. SLAC Report No. 281: 513, 1985. See also Crystal Ball Collaboration, "Evidence for Narrow Massive State in the Radiative Decays of the Upsilon", SLAC-PUB-3380, 1984.
33. B. Schwarzchild, *Physics Today*, p. 19, March 1985.
34. G. Arnison *et al.* [UA1 Collaboration], Phys. Lett. B **147** (1984) 493.
35. S. Stepanyan *et al.* [CLAS Collaboration], Phys. Rev. Lett. **91** (2003) 252001.
36. K. Hicks, J. Phys. Conf. Ser. **9** (2005) 183.
37. K. H. Hicks, Eur. Phys. J. H **37** (2012) 1.
38. R. A. Schumacher, AIP Conf. Proc. **842** (2006) 409.
39. A. Roodman, eConf C **030908** (2003) TUIT001.
40. J. R. Klein and A. Roodman, Ann. Rev. Nucl. Part. Sci. **55** (2005) 141, 2005.
41. G. L. Bayatian *et al.* [CMS Collaboration], J. Phys. G **34** (2007) 995.
42. A. Czarnecki, J. G. Korner and J. H. Piclum, Phys. Rev. D **81** (2010) 111503.
43. M. Jacob and G. C. Wick, Annals Phys. **7** (1959) 404.
44. J. D. Richman. Caltech Preprint CALT-68-1148, 1986.
45. S. Chatrchyan *et al.* [CMS Collaboration], Eur. Phys. J. C **73** (2013) 2404.
46. CMS Collaboration. Search for supersymmetry in pp collisions at a center-of-mass energy of 8 TeV in events with a single lepton, multiple jets and b-tags. CMS PAS-SUS-13-007, 2013.
47. Z. Bern *et al.*, Phys. Rev. D **84** (2011) 034008.
48. Z. Bern *et al.*, Phys. Rev. D **87** (2013) 3, 034026.
49. G. L. Kane, C. F. Kolda, L. Roszkowski and J. D. Wells, Phys. Rev. D **49** (1994) 6173.
50. A. H. Chamseddine, R. L. Arnowitt and P. Nath, Phys. Rev. Lett. **49** (1982) 970.
51. J. A. Conley *et al.*, Eur. Phys. J. C **71** (2011) 1697.
52. J. A. Conley *et al.*, arXiv:1103.1697 [hep-ph].
53. N. Arkani-Hamed *et al.*. hep-ph/0703088 [HEP-PH].
54. J. Alwall, P. Schuster and N. Toro, Phys. Rev. D **79** (2009) 075020.
55. J. Alwall, M. -P. Le, M. Lisanti and J. G. Wacker, Phys. Rev. D **79** (2009) 015005.
56. D. Alves *et al.* [LHC New Physics Working Group Collaboration], J. Phys. G **39** (2012) 105005.
57. H. P. Nilles, Phys. Rept. **110** (1984) 1.
58. P. Fayet, Phys. Lett. B **70** (1977) 461.
59. H. Baer, M. Brhlik, C. -h. Chen and X. Tata, Phys. Rev. D **55** (1997) 4463.
60. H. Baer, P. G. Mercadante, X. Tata and Y. -l. Wang, Phys. Rev. D **60** (1999) 055001.
61. S. Dimopoulos, S. D. Thomas and J. D. Wells, Nucl. Phys. B **488** (1997) 39.
62. J. R. Ellis, J. L. Lopez and D. V. Nanopoulos, Phys. Lett. B **394** (1997) 354.

63. M. Dine, A. E. Nelson, Y. Nir and Y. Shirman, Phys. Rev. D **53** (1996) 2658.
64. G. F. Giudice and R. Rattazzi. in *Perspectives on Supersymmetry*, p. 355 (World Scientific, Signature, 1998).
65. P. Meade, N. Seiberg and D. Shih, Prog. Theor. Phys. Suppl. **177** (2009) 143.
66. M. Buican, P. Meade, N. Seiberg and D. Shih, JHEP **0903** (2009) 016.
67. G. R. Farrar and P. Fayet, Phys. Lett. B **76** (1978) 575.
68. W. Beenakker, S. Brensing, M. Kramer, A. Kulesza, E. Laenen and I. Niessen, JHEP **1008** (2010) 098.
69. W. Beenakker, S. Brensing, M. Kramer, A. Kulesza, E. Laenen, L. Motyka and I. Niessen, Int. J. Mod. Phys. A **26** (2011) 2637.
70. M. Kramer, A. Kulesza, R. van der Leeuw, M. Mangano, S. Padhi, T. Plehn and X. Portell, arXiv:1206.2892 [hep-ph].
71. G. Aad *et al.* [ATLAS Collaboration], Eur. Phys. J. C **72** (2012) 1844.
72. C. G. Lester and D. J. Summers, Phys. Lett. B **463** (1999) 99.
73. A. Barr, C. Lester and P. Stephens, J. Phys. G **29** (2003) 2343.
74. S. Chatrchyan *et al.* [CMS Collaboration], Phys. Rev. Lett. **111** (2013) 081802.
75. [ATLAS Collaboration], ATLAS-CONF-2012-147.
76. G. Aad *et al.* [ATLAS Collaboration], Phys. Rev. Lett. **110** (2013) 011802.
77. [CMS Collaboration], CMS-PAS-EXO-12-048.
78. B. Gomber [CMS Collaboration], Phys. Rev. Lett. **108** (2012) 261803.
79. Y. Bai, P. J. Fox and R. Harnik, JHEP **1012** (2010) 048.
80. A. Rajaraman, W. Shepherd, T. M. P. Tait and A. M. Wijangco, Phys. Rev. D **84** (2011) 095013.
81. L. Randall and D. Tucker-Smith, Phys. Rev. Lett. **101** (2008) 221803.
82. [CMS Collaboration], CMS-PAS-SUS-12-028.
83. S. Chatrchyan *et al.* [CMS Collaboration], Phys. Rev. Lett. **109** (2012) 171803.
84. [ATLAS Collaboration], ATLAS-CONF-2012-104.
85. D. S. M. Alves, M. R. Buckley, P. J. Fox, J. D. Lykken and C. -T. Yu, Phys. Rev. D **87** (2013) 3, 035016.
86. S. Chatrchyan *et al.* [CMS Collaboration], JHEP **1303** (2013) 037 [Erratum-ibid. **1307** (2013) 041].
87. [ATLAS Collaboration], ATLAS-CONF-2012-105.
88. H. Davoudiasl, J. L. Hewett and T. G. Rizzo, Phys. Rev. D **63** (2001) 075004.
89. M. J. Strassler and K. M. Zurek, Phys. Lett. B **651** (2007) 374.
90. T. Han, Z. Si, K. M. Zurek and M. J. Strassler, JHEP **0807** (2008) 008.
91. N. Arkani-Hamed and S. Dimopoulos, JHEP **0506** (2005) 073.
92. N. Arkani-Hamed, S. Dimopoulos, G. F. Giudice and A. Romanino, Nucl. Phys. B **709** (2005) 3.
93. V. Khachatryan *et al.* [CMS Collaboration], Phys. Rev. Lett. **106** (2011) 011801.
94. S. Chatrchyan *et al.* [CMS Collaboration], JHEP **1307** (2013) 178.